Clean Energy and Sustainability

SCIEPublish

Article

# Feasibility Study of Designing a Sustainable Off-Grid Solar Photovoltaic System for Household Power Generation

**Vincent Anayochukwu Ani [1,2,*] and Mustapha Abdullahi [2]**

[1] National Centre for Energy Research and Development, University of Nigeria, Nsukka 410105, Nigeria
[2] Energy Commission of Nigeria, Abuja 900107, Nigeria

* Corresponding author. E-mail: aavincent@energy.gov.ng (V.A.A.)

Received: 23 May 2026; Revised: 2 July 2026; Accepted: 21 September 2026; Available online: 27 October 2026

**ABSTRACT:** Household solar photovoltaic (SPV) systems often experience failures shortly after installation, primarily due to design deficiencies. Consequently, systems composed of well-designed, high-quality components installed by professionals can maintain efficiency and ensure long-term profitability. This study presents a methodology for accurately sizing an off-grid SPV system to ensure reliable electricity generation. A mathematical model was employed to assist in the design of an SPV system that consistently meets energy demands. A stochastic approach was developed using the hybrid optimization of multiple energy resources (HOMER) Pro software (version 3.18.4) to accurately design and predict the performance of the SPV system. This approach incorporates time-series data to model the inherent uncertainty and variability associated with solar resources and load demands. A sensitivity analysis was performed to evaluate the effects of variations in solar irradiance and load growth on system performance. The findings suggest that the proposed system methodology is applicable to other regions of Nigeria and other developing countries with different climatic conditions and load profiles. The insights and findings presented in this study could assist the Energy Commission of Nigeria (ECN) in developing policies for deploying solar-powered household systems across Nigeria. A potential policy could require prospective clients intending to install SPV systems for household electricity generation to submit a pre-feasibility study. This study should include the residential load profile, solar irradiation of the location, and appropriate system sizing. Such a requirement should precede the approval of any physical project proposal to reduce system failures in PV systems in Nigeria.

**Keywords:** Energy Commission of Nigeria; Off-grid SPV systems; HOMER software; Stochastic approach; Sensitivity analysis; LPSP

## 1. Introduction

Energy, especially electrical energy, is a crucial determinant of living standards in any country, and its provision constitutes a fundamental component of the Sustainable Energy for All (SE4ALL) initiative. The demand for electricity is progressively increasing due to contemporary living standards. It plays a vital role in improving the quality of life, especially in rural areas. Solar power, which is universally accessible, is

© 2026 The authors. This is an open access article under the Creative Commons Attribution 4.0 International License (https://creativecommons.org/licenses/by/4.0/).

particularly appealing for comprehensive systems in rural Nigeria [1]. Despite Nigeria's substantial renewable energy potential, the country continues to face persistent energy challenges. In response, the Energy Commission of Nigeria (ECN) is actively promoting a transition to sustainable energy through renewable sources to supply electricity to off-grid rural communities [2]. According to the ECN boss, solar energy is a strategic focus, leveraging the country's favourable solar radiation to implement widespread solarization [2]. Nigeria's daily global horizontal radiation varies from 4.8 kWh/m$^2$/day (26.5 MJ/m$^2$/day) to 7.0 kWh/m$^2$/day (15.7 MJ/m$^2$/day), with an average daily solar irradiation duration of 7.5 h [3]. The country has ample solar energy potential to address its energy challenges and enhance rural electrification. However, the deployment of off-grid solar photovoltaic (SPV) systems is significantly hindered by their failure. The primary causes of off-grid SPV system failures include improper system sizing, the use of substandard and low-quality components, inadequate installation practices by untrained technicians, and insufficient maintenance. Among these, improper system sizing has been identified as the primary cause of premature failures in off-grid SPV systems in Nigeria. There is often a substantial discrepancy between the actual energy consumption of Nigerian households and the capacity of the installed systems, resulting in overloads, rapid battery degradation, and eventual system abandonment. The prevalence of substandard and low-quality components, such as panels, inverters, and batteries, is a significant factor contributing to the failure of off-grid SPV systems in Nigeria. This issue results in a high incidence of premature system breakdowns, safety hazards, and a decline in consumer confidence. Suppliers frequently import low-cost counterfeit components to maximize profits. These include low-efficiency panels, batteries with short lifespans, and inverters prone to malfunction at elevated temperatures. Furthermore, inadequate installation practices are a major cause of premature failure of off-grid SPV systems in Nigeria. Although low-quality components exacerbate this problem, even high-quality equipment is susceptible to failure if improperly installed, potentially leading to short circuits, fire hazards, and reduced system longevity. Poor installation practices by untrained technicians have led to SPV system failures and performance losses due to mismatches, hotspots, and bypass diode issues [4]. Consequently, a system comprising well-designed, high-quality components installed by professionals can sustain efficiency and ensure long-term profitability.

### *SPV System Reliability*

The reliability of SPV systems is a critical research domain aimed at ensuring that solar power plants function efficiently, safely, and with minimal interruptions over their projected lifespan of 25 years or more [5]. Recent advancements have focused on the integration of artificial intelligence (AI) for real-time fault detection, application of phase-change materials (PCM) for thermal management to sustain high efficiency, and employment of dynamic simulation tools to optimize power output [6–8]. Advanced modelling techniques for SPV systems are currently employed to predict power output, diagnose faults, and evaluate the reliability of these systems under complex and variable environmental conditions. Nonetheless, the sizing of system components remains a significant technical challenge in the design of off-grid SPV systems [9].

The reliability of the power supply is a critical consideration in the design of PV/battery systems, as evidenced by its inclusion in specific sizing procedures. The reliability of power supply to a load is defined as the probability that the system functions correctly over a specified period under operational conditions without failure. This study emphasizes the necessity of designing an optimal PV/battery system that exhibits enhanced reliability and appropriately addresses technical objectives. Among the various technical objectives employed by researchers, such as loss-of-power supply probability (LPSP) [10] and loss-of-load probability [11], this study focuses on LPSP as the chosen technical objective. LPSP, a probabilistic technique introduced by [12], is extensively utilized in the design and optimization of renewable energy generation systems. It is calculated based on the variability of resources and their correlation with the loads. This method is particularly effective for evaluating the performance of energy storage systems, as demonstrated in this study.

## 2. Off-Grid SPV Systems Review

Off-grid SPV systems are predominantly utilized in remote areas, where the cost of connecting to the utility grid surpasses that of acquiring an off-grid system [13]. In these systems, a solar electric configuration serves as the primary power source for residences and comprises solar panels, an inverter, a battery bank, and a charge controller. Solar electric-based off-grid systems are increasingly being adopted to meet the electricity needs of rural households and are of significant interest for rural electrification. However, the sizing of these systems presents challenges, as it requires aligning unpredictable energy sources with uncertain demand while ensuring optimal reliability [14]. In Nigeria, the demand for solar electric systems for residential applications is increasing. To achieve optimal system design, it is crucial to utilize a suitable calculation method that accounts for the specifications and sizing of each component of the solar electric generation system. Furthermore, a storage system is essential for an off-grid SPV system to provide continuous electricity for 24 h. The battery bank functions as a backup power source to meet the demand load during the morning and evening periods.

Numerous off-grid initiatives targeting households have been unsuccessful because of errors in system sizing. Such mistakes are prevalent in off-grid SPV systems, especially when deployed for residential purposes. Many installed systems exhibit design flaws that lead to frequent outages, primarily due to sizing errors [15]. According to [16], almost half of all installed systems have design issues that result in recurrent outages. Nigerian consumers invest substantial amounts in installing SPV systems in residential structures, including duplexes, single-family bungalows, flat apartments, and "face-me-I-face-you" configurations for electricity generation. These systems frequently fail shortly after installation, potentially due to technical issues. Technical factors pertaining to system design and sizing directly impact the reliability of SPV systems. To evaluate the technical performance of a stand-alone SPV system, it is essential to determine the sizes of its components. Stand-alone SPV systems are designed to satisfy daily load demand rather than annual demand [17]. Consequently, each component of the SPV system must be carefully sized to meet this requirement [18]. Determining the capacity of the SPV array, including the quantity and wattage of the PV modules, is essential to ensure the power generated is sufficient to fully charge the battery bank [19]. Consequently, precise calculations are required to determine the size of the battery bank capable of continuously supplying electrical power to the load during nighttime or periods of low solar radiation [17]. Therefore, in addition to considering the battery type and parameters, the average daily load is a critical factor in determining the battery bank size [20]. The capacity of a PV array is generally influenced by the daily load and solar radiation at the study site [18]. These factors must be thoroughly evaluated during the design process to avoid oversizing or undersizing stand-alone systems. These factors assist planners in designing suitable systems that can be practically applied in specific environments; ignoring them will result in a non-functional system. They play a crucial role in sizing SPVs. Adewuyi [21] conducted a survey on SPV systems in residential buildings and discovered that malfunctions and failures were due to incorrect sizing.

This study indicates that while many studies emphasize load profiles and solar resources, they often lack a thorough examination of the sizing of SPV systems. This study provides a comprehensive design and sizing plan for household SPV systems. The goal of this study was to evaluate the technical feasibility of designing off-grid SPV systems to provide electricity to residential buildings. Additionally, it aims to offer precise data to support the development of a policy framework for the installation of off-grid SPV systems in Nigeria.

### *Sizing Techniques for SPV System*

Different methodologies have been proposed for sizing off-grid SPV systems, as indicated by a review of existing literature. Among these, analytical, numerical, and intuitive methods are the most commonly employed [9,22]. These methodologies can be complemented by computer simulations to determine the optimal size of an off-grid SPV system.

Numerous intuitive approaches have been devised for the optimal sizing of standalone PV systems. Ahmad [23] introduced an intuitive method for determining the optimal size of the PV/battery configuration in standalone PV systems for remote residences in Egypt. The design process commenced with the calculation of the average daily load demand and solar radiation. Using straightforward mathematical equations, the dimensions of the PV array and storage battery capacity were determined. The selection of the battery charge controller and inverter was based on the extended lifespan and maximum anticipated power. However, the reliability level, which could result in over-or under-sizing of the design, was not considered in the sizing of the standalone PV system. Al-Salaymeh [24] conducted an optimal sizing study of a standalone PV system for residential buildings in Jordan using an intuitive method. This study utilized daily averages of meteorological and load demand data. The sizing process commenced with the calculation of the average daily load energy requirements, followed by the determination of the PV array size using peak sun hours (PHS). However, this study did not account for the technical and economic aspects of sizing the PV array and the storage battery, which could lead to oversizing. Furthermore, reliance on daily average data may yield inaccurate results, potentially compromising system reliability. Kaushika and Rai [25] introduced an intuitive method for determining the PV array and batteries in standalone PV system, specifically for certain regions in India. This method was utilized to develop an expert system that operates based on geographical coordinates. By using monthly average solar energy data alongside site coordinates, the system aims to optimize the tilt angle. However, this expert system may not match the efficiency of contemporary software tools that employ more precise optimization techniques. Furthermore, this method does not incorporate technical and economic considerations for sizing standalone PV systems. These reviews indicate that the intuitive method offers a simplified approach to calculating system components, particularly the size of an SPV system, without accounting for the stochastic nature of solar radiation, electricity consumption patterns, or interactions among subsystem components. This method is best suited for initial approximations or estimations of the system, although it may result in excess or insufficient solar energy production.

Simulation-based methods, also known as numerical methods, are categorized into stochastic and deterministic approaches. These methods provide more precise and detailed sizing by simulating uncertainties related to variations in solar resources and load demands. In the stochastic approach, uncertainties are modelled using hourly demand and insolation data, whereas the deterministic approach uses daily averages for both demand and insolation data [9]. A review of the literature indicates that the numerical approach is more accurate than the intuitive method, as it incorporates system simulation and mathematical modeling for optimization rather than relying solely on rough estimates.

In the analytical approach, simple mathematical equations are often used to determine the optimal size of an SPV system and battery storage based on reliability [22]. Nevertheless, the performance of the proposed system can be further assessed through computer simulations, which are conducted after deriving a simplified mathematical equation to ascertain the optimal values for the PV and battery [18]. Research indicates that computer simulation tools, such as the Hybrid Optimization of Multiple Energy Resources (HOMER) Pro software (version 3.18.4), are more effective in evaluating the performance of off-grid SPV systems [26]. This study examined the stochastic characteristics of electricity consumption patterns in the context of sizing off-grid SPV systems for residential applications. Previous studies have not adequately addressed the dynamic nature of residential load profiles in these regions. The stochastic nature of electricity consumption, characterized by hourly demand, renders the numerical method the most effective sizing technique for this design. Therefore, the sizing of an off-grid SPV system for a sustainable household power supply was conducted using a numerical method, which was verified using a computer program. This study contributes to existing knowledge by introducing a novel approach for the optimal sizing of off-grid SPV systems.

## 3. Design Concept

This study evaluated the feasibility of designing an off-grid SPV system for households in southeastern Nigeria. The primary objective was to appropriately size the PV/battery system components to meet household energy demand and establish a procedure for designing such a system. The development and design processes of the system included the following steps:

- Identify the household's energy service requirements.
- Design an energy system that fulfills the household's energy needs by accurately sizing each subsystem.
- Utilize HOMER software to design the SPV system and calculate its life-cycle cost, operating cost, and levelized cost of electricity.
- Provide useful information that could inform policy frameworks for installing SPV systems in Nigeria.

### *3.1. Solar Energy Potential and Insolation*

Akpugo is located within Nkanu-West local government area of Enugu State, Nigeria. Akpugo, like all other Igbo clans, is situated in the savannah region of the former Eastern Nigeria, with coordinates spanning latitudes 6.20° to 6.25° N and longitudes 7.34° to 7.39° E. It is bordered to the north by Agbani, to the south by Emene, to the east by Ugwuaji, and to the west by Amagunze. The Akpugo community includes Oriemba, Ndiagu Akpugo, Onuafo, Akpawfu, and Ugwuafor [27]. The geographical and meteorological data for the solar system in Ndiagu Akpugo (Figure 1) were sourced from the NASA Surface Meteorology and Solar Energy (NASA-SSE) site database and compared with data generated from the HOMER software (Figure 5). The meteorological data, which illustrate the average monthly solar irradiance used in this study, are shown in Figure 1.

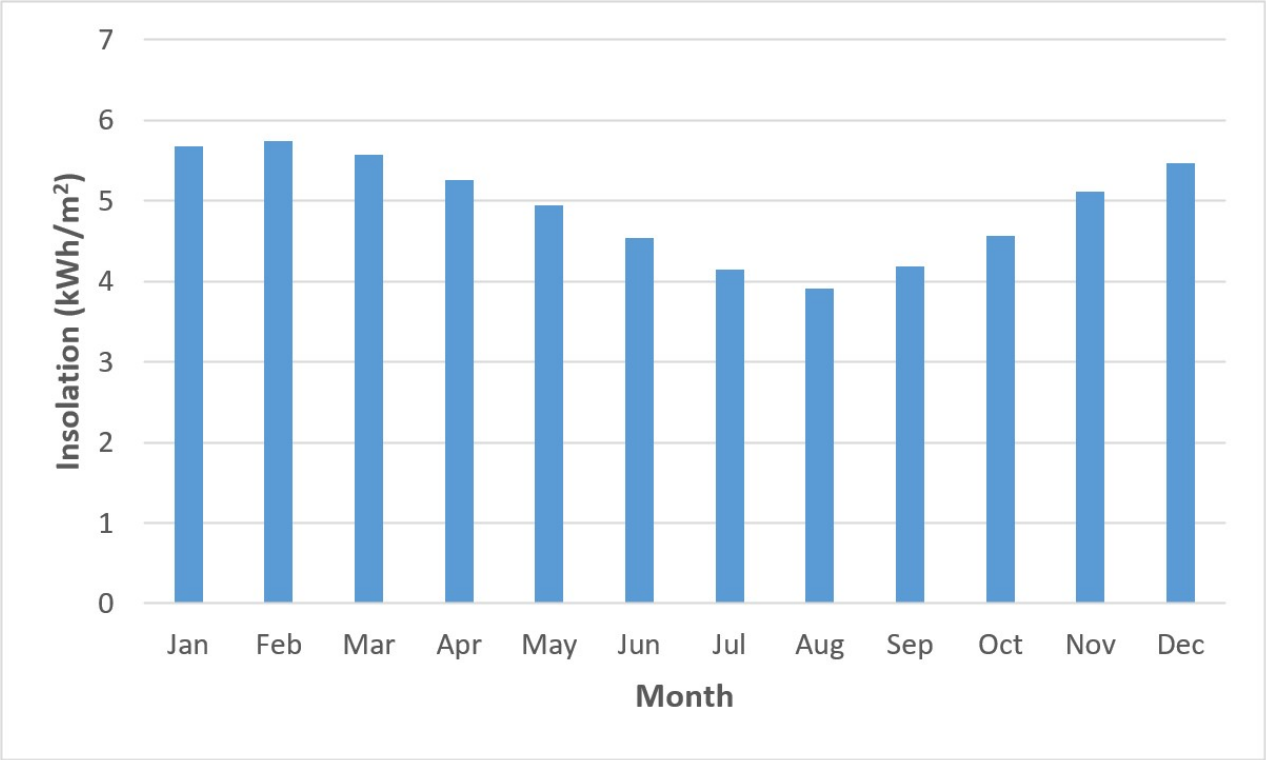



**Figure 1.** Monthly insolation in Ndiagu, Akpugo.

Solar Resource Variation

In the analysis of solar radiation variation, February was identified as the month with the highest solar exposure, characterized by a solar energy resource of 5.7 kWh/m$^2$/day, as indicated in Figure 1. Conversely, August exhibited a lower solar energy resource of 3.9 kWh/m$^2$/day. In August, the battery can provide compensation. From September to February, solar radiation progressively increased, with monthly increments of 0.28, 0.38, 0.54, 0.35, 0.22, and 0.06, respectively. In contrast, from March to August, solar radiation declined, with monthly decreases of 0.17, 0.32, 0.31, 0.4, 0.4, and 0.23, respectively. During these months, the battery can provide compensation.

### *3.2. Off-Grid SPV System*

An off-grid SPV system comprises a PV module array, solar charge controller, battery bank, and inverter to convert the generated direct current (DC) into alternating current (AC) power. The sizing of this system was based on the daily energy loads and energy potential of the area. These parameters were used to ascertain the capacity and specifications of each component of the solar electric system.

### *3.3. Energy Service Requirements of the Household*

Household energy demands are categorized into two types: residential load consumption, which refers to the daily load profile (primary load), and water pumping systems, which are classified as deferrable loads.

#### 3.3.1. Residential Load Consumption—Daily Load Profile

Electricity is recognized as a powerful tool for improving living conditions through services such as lighting, heating, cooling, and production [13]. The residential load consumption of a household includes essential electrical devices such as light bulbs for lighting, ceiling fans, a television set, a decoder, a refrigerator, a deep freezer, and a water pump. The operation of these devices depends on the resident's preferences and lifestyle. To determine the daily energy consumption pattern, the electrical requirements of the household were estimated. The power ratings of the appliances used each hour over a 24-h period were summed, and this total was converted into kilowatt-hours (kWh) by dividing by 1000. Table A1 in Appendix A and Figure 2 illustrate the daily load profile.

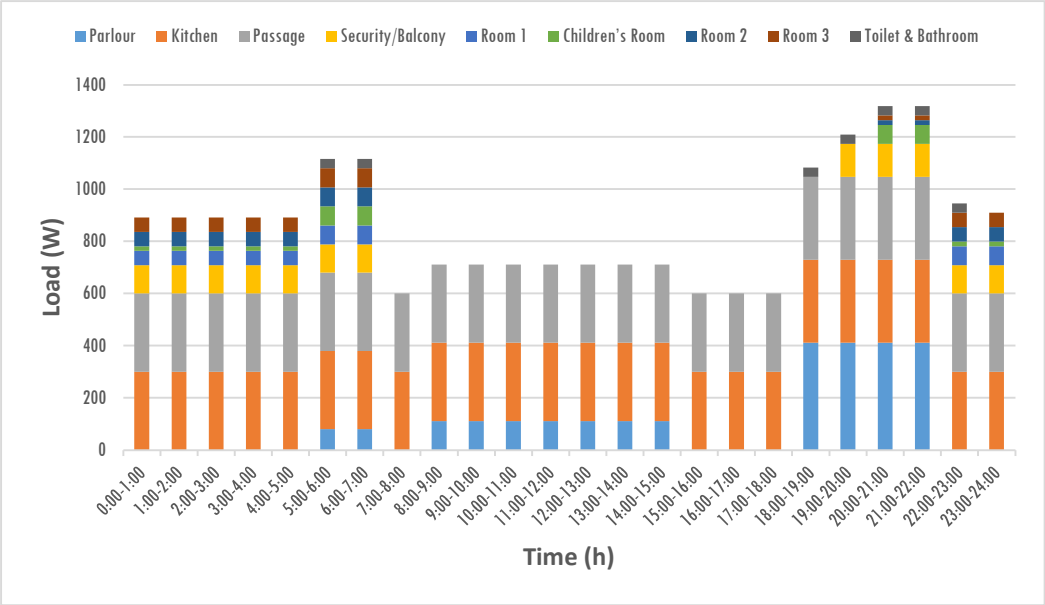



**Figure 2.** Load profile of the house.

### 3.3.2. Water Pumping System—Deferrable Load

Incorporating water pumping into the design accurately reflects residential energy consumption patterns. This household requires approximately 3.3 $m^3$ of water daily and utilizes a borehole with a total differential head (TDH) of 90.6 m. Subsequently, the water demand was increased to 5.2 $m^3$ per day to accommodate an additional 1.9 $m^3$ intended for sale to water vendors. The water storage system comprised a plastic tank with a height of 2.5 m and a volume of 10 $m^3$. With an irradiance of 3.9 kWh (Figure 1), a water flow rate of 2.6 $m^3$ per hour was achieved. A submersible pump capable of lifting 10,000 litres of groundwater per day was found to require 1.094 kW (Figure 3). According to the water usage calculations, 5.2 $m^3$ of water will be produced daily, with 3.3 $m^3$ allocated to the household and the remaining 1.9 $m^3$ designated for sale to water vendors.

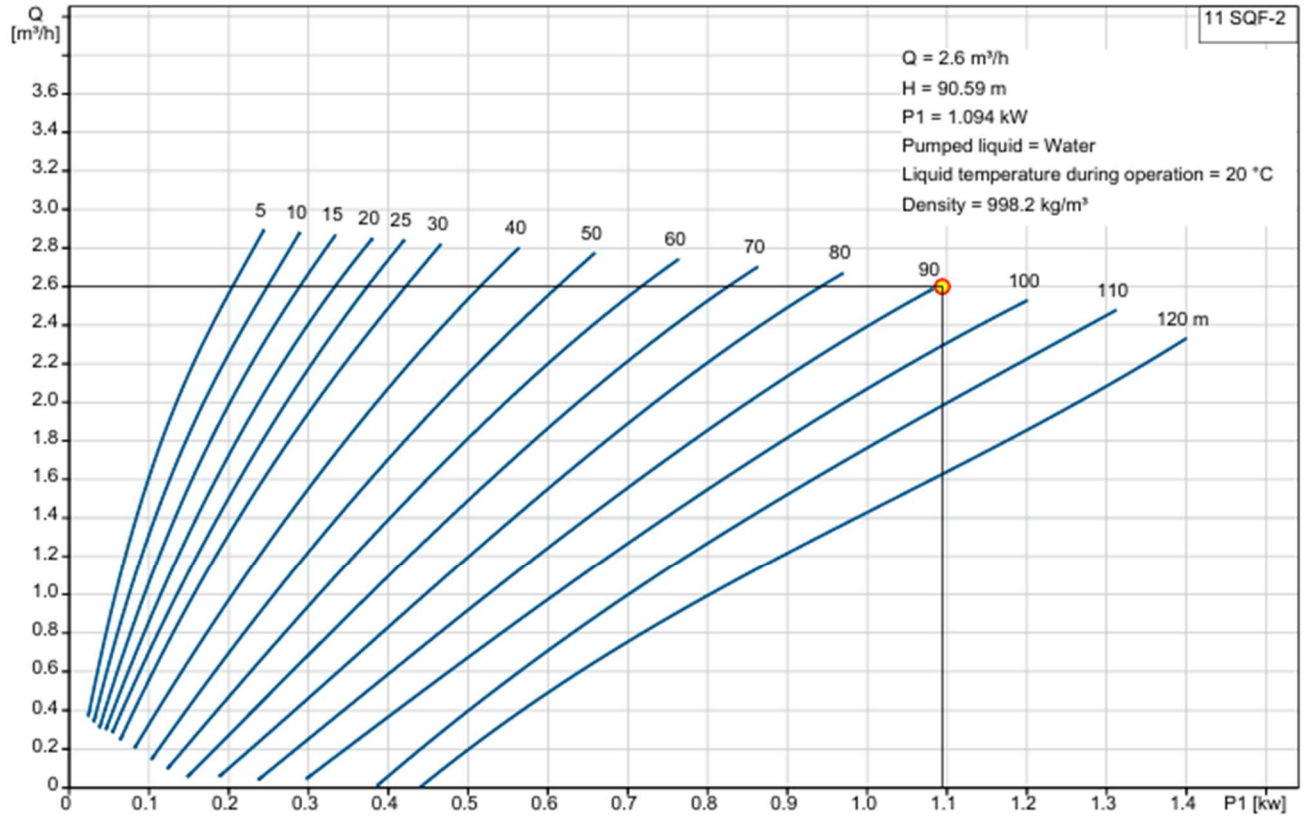



**Figure 3.** Pump performance curve for Grundfos 11 SQF–2 Solar Submersible System.

### Pump Sizing

The duration (in hours) required for the pump to fill a 10 $m^3$ water tank was determined by:

$$\text{Time (h)} = \frac{\text{volume of water tank } (m^3)}{\text{water flow rate } (m^3/h)} = \frac{10\ m^3}{2.6\ m^3/h} = 3.9\ h$$

Therefore, the pump will require 3.9 h to fill the tank.

$$\text{Storage Capacity} = \text{time} \times \text{rated power of the pump} = 3.9\ h \times 1.094\ kW = 4.267\ kWh$$

Subsequently, the time (h) required for the pump to fulfill the daily water requirement was determined by:

$$\text{Time (h)} = \frac{\text{daily water requirement } (m^3)}{\text{water flow rate } (m^3/h)} = \frac{5.2\ m^3}{2.6\ m^3/h} = 2\ h$$

The pump will require 2 h to meet the daily water requirement.

$$\text{Daily Pump Load} = \text{time} \times \text{rated power of the pump} = 2\ \text{h} \times 1.094\ \text{kW} = 2.188\ \text{kWh}$$

$$\text{Pump Peak Load} = \text{rated power of the pump} = 1.094\ \text{KW}$$

The Grundfos 11 SQF-2 solar submersible pump operates at a minimum of 8.4 A to serve the deferrable load, which corresponds to a 30 V DC bus with a minimum power of $P_{min} = 0.25$ kW [28,29]. The minimum power required to serve the pump load is calculated as follows:

$$\text{Minimum Load Ratio (\%)} = \left[\frac{\text{minimum power of the pump}}{\text{pump peak load}}\right] \times 100\% = \left[\frac{0.25}{1.09}\right] \times 100 = 22.94\%$$

### *3.4. Individual Sizing of Subsystems*

To enhance the flexibility of the system, each subsystem was independently sized. The subsystems of the off-grid SPV system were sized as follows:

- The PV array subsystem serves as the generation unit.
- The solar charge controller subsystem, which acts as the energy control unit, regulates the current and voltage flow into the battery and DC appliances.
- The inverter subsystem functions as the electrical energy conversion and distribution unit for electrical loads.
- The battery bank subsystem acts as a storage unit that stores the energy generated by the PV array.

This sizing process considers factors such as the daily sun hours at the location, the system's DC input voltage, the number of days the battery can supply power in the absence of solar radiation, the wattage of load devices along with their daily operation duration, and the specifications of the PV module, with the duration of their daily operation, and the PV module's specifications. A series of design equations can be employed to manually design an SPV system. These equations were obtained from the literature [30].

#### 3.4.1. Sizing of the PV Array System

The total size of the PV array was determined by considering the total daily energy demand, the lowest irradiation value expressed in peak sun hours (PSH), and the losses incurred in each component of the standalone SPV system, including the charge controller, battery, and inverter, as illustrated in Equation (1). The total size of the PV array was calculated as follows:

$$T_{PV} = \left[\left[\frac{AC_{LOAD}}{(PSH_{lowest} \times \eta_{cc} \times \eta_{batt} \times \eta_{inv})}\right] + \left[\frac{DC_{LOAD}}{(PSH_{lowest} \times \eta_{cc})}\right]\right] \times 1.25 \quad (1)$$

$$\therefore T_{PV} = \left[\left[\frac{20{,}954}{(3.91 \times 0.95 \times 0.96 \times 0.95)}\right] + \left[\frac{2188}{(3.91 \times 0.95)}\right]\right] \times 1.25 = 8468.1\ \text{W}$$

where:
$T_{PV}$ is the total size of a PV array rated in Watt peak (Wp)
$AC_{LOAD}$ is the total AC daily energy demand in Wh
$PSH_{lowest}$ is the month with the lowest peak sun hours of the study location
$\eta_{cc}$ is the efficiency of the charge controller
$\eta_{batt}$ is the efficiency of the battery
$\eta_{inv}$ is the efficiency of the inverter
$DC_{LOAD}$ is the total DC daily energy demand in Wh
1.25 is the safety factor

A monocrystalline PV module with a peak power rating of 415 Wp was selected for the standalone SPV system. The module specifications are listed in Table 1.

**Table 1.** Topsun Monocrystalline Solar Module.

| **Module Models** | **TS-S415** |
|---|---|
| Maximum power point ($P_{max}$) | 415 Wp |
| Maximum power point voltage ($V_{mpp}$) | 48.49 V |
| Maximum power point current ($I_{mpp}$) | 8.56 A |
| Open circuit voltage ($V_{oc}$) | 60.45 V |
| Short circuit current ($I_{sc}$) | 9.04 A |
| Temperature coefficient ($TCV_{oc}$) | −0.33 %/°C |
| Normal operating cell temperature (NOCT) | 45 °C |

The total number of PV modules required to meet the energy demand was calculated by dividing the total capacity of the PV array by the maximum power output of the unit PV array, as expressed in Equation (2).

$$TN_{PV} = \frac{T_{PV}}{P_{max}} = \frac{8468}{415} = 20.4 \approx 21 \text{ modules} \quad (2)$$

where:
$TN_{PV}$ is the total number of PV modules
$P_{max}$ represents the maximum power output of the unit PV array.

To identify the best PV string configuration for the system, it is essential to configure a series and parallel connection of modules that sum up to 21, while meeting the voltage criteria for a nominal 48 V battery bank. To achieve an even distribution of 21 solar panels in balanced configurations, a setup was chosen where each string contained an equal number of panels. Given that 21 is a composite number with distinct integer factors of 3 and 7, the array can be configured as either a high-voltage, low-current system (7 series × 3 parallel) or as a mid-voltage, high-current system (3 series × 7 parallel). The selected configuration was 3S7P, comprising three modules connected in series and seven strings in parallel. This decision was informed by the charge controller's constraints, which include a maximum DC input voltage of 250 V and a maximum short-circuit current of 100 A. Table 2 presents the specifications for a 250 V/100 A maximum power point tracking (MPPT) charge controller. Equation (3) was used to calculate the total voltage of the PV input series:

$$SV_{oc} = N_s \times V_{oc} = 3 \times 60.45 \text{ V} = 181.35 \text{ V} \quad (3)$$

Equation (4) is used to calculate the total current of the PV input in parallel:

$$PI_{sc} = N_p \times I_{sc} = 7 \times 9.04 \text{ A} = 63.28 \text{ A} \quad (4)$$

This configuration results in the $V_{mpp}$ of 145.47 V $(3 \times SV_{mpp} = 3 \times 48.49)$ and an open-circuit voltage of 181.35 V $(3 \times V_{oc} = 3 \times 60.45)$, offering a perfect voltage margin to safely and effectively charge a nominal 48 V battery bank using standard 250 V MPPT charge controllers, which are widely available. The open-circuit voltage of 181.35 V of the 3S7P array operates seamlessly with a 250 V controller. As solar panel voltages increase with decreasing ambient temperature, the 3S7P setup maintains a secure margin below 250 V during cold mornings. Furthermore, the $I_{mpp}$ was 59.92 A $(7 \times SI_{mpp} = 7 \times 8.56 \text{ A})$, and its short-circuit current was 63.28 A $(7 \times I_{sc} = 7 \times 9.04 \text{ A})$. With a very high current of 63.28 A, this system is compatible with mid-voltage charge controllers rated at 250 V.
Where:
$N_S$ represents the number of panels that must be connected in series
$SV_{oc}$ denotes the series voltage
$V_{oc}$ is the open circuit voltage
$SV_{mpp}$ indicates the string operating voltage
$V_{mpp}$ is the maximum power point voltage

$N_P$ refers to the number of panels that must be connected in parallel
$PI_{sc}$ is the parallel current
$I_{sc}$ is the short circuit current
$SI_{mpp}$ is the string operating current
$I_{mpp}$ is the maximum power point current

### 3.4.2. Sizing of Solar Charge Controller

The primary function of a solar charge controller is to regulate the voltage and current from the PV panels to the battery, thereby preventing overcharging and prolonging the battery life. Table 2 lists the electrical specifications of the 250 V/100 A MPPT charge controller.

**Table 2.** Electrical specifications of 250 V/100 A MPPT charge controller.

| Solar PV Input Specifications | Battery Output Specifications |
|---|---|
| Maximum open-circuit voltage ($V_{oc}$): 250 V | Nominal battery voltage: 48 V |
| Maximum short-circuit current ($I_{sc}$): 70 A | Maximum charging current: 100 A |

To allocate the 21 modules among several standard MPPT charge controllers, seven parallel strings must be distributed evenly. Given that seven is a prime number, it is not feasible to divide a single 3S7P array into two equal sections. Consequently, two standard MPPT controllers were utilized, partitioning the array into 3S4P and 3S3P sub-arrays (Table 3). The use of two 250 V/100 A controllers (MPPT 1 and 2) ensures optimal voltage regulation and provides substantial system redundancy. Equation (5) is used to connect two MPPT configurations:

$$TM_c = [(3S \times 4P) + (3S \times 3P)] \quad (5)$$

where $TM_c$ is the total PV modules connected.

**Table 3.** Two-MPPT connection configuration

| Parameter | MPPT 1 (3S4P Sub-Array) | MPPT 2 (3S3P Sub-Array) |
|---|---|---|
| Total Modules Connected | 12 modules (3S × 4P) | 9 modules (3S × 3P) |
| Max PV Voltage ($V_{oc}$) | 181.35 V | 181.35 V |
| Total PV Input Current ($I_{sc}$) | 36.16 A (4 × 9.04 A) | 27.12 A (3 × 9.04 A) |

### 3.4.3. Sizing of the Battery Bank

The "days of autonomy" is a critical factor in determining the appropriate size of battery units, in conjunction with the nominal voltage and depth of discharge of the battery. Batteries play a vital role in storing the output power of PV arrays to satisfy power demands during nighttime or prolonged cloudy conditions. A three-day autonomy period was selected for the household off-grid power systems to ensure reliable backup during extended severe weather or low-solar events. The technical justification for selecting a three-day (72-h) autonomy period is to balance reliability against high equipment costs, as the household user cannot tolerate power losses. This system is intended for installation in southern Nigeria, where multi-day weather anomalies occur, in contrast to the consistently sunny conditions in northern Nigeria. The 72-h autonomy period accommodates a complete human and electrical routine, encompassing overnight base loads, morning peaks, and daytime use without external supply or generation. The capacity of the battery bank, which specifies the size requirement based on the estimated usage, can be calculated using Equation (6):

$$C_{T,batt} = \left[\frac{(1.25 \times AC_{LOAD})}{(DOD \times \eta_{inv} \times V_{DC})}\right] \times n = \left[\frac{(1.25 \times 20{,}954)}{(0.80 \times 0.95 \times 48)}\right] \times 3 = 2154.0 \approx 2154\ Ah \quad (6)$$

where:

1.25 is the safety factor
$C_{T,batt}$ is the total battery capacity in Ampere hours
n is the number of autonomy days
DOD is the depth of discharge of the battery; it indicates the maximum amount of charge that can be discharged from a battery

A lithium iron phosphate battery with a nominal capacity of 400 Ah at 12 V was selected for the standalone SPV system. The specifications are listed in Table 4.

**Table 4.** A standard 12 V 400 Ah lithium iron phosphate ($LiFePO_4$) battery.

| **Battery Type** | **$LiFePO_4$ (12 V, 400 Ah)** |
|---|---|
| Nominal capacity | 400 Ah |
| Nominal Voltage | 12 V |
| Cycle lifespan | >3000 cycles @ 80% DOD |
| Efficiency | 96% |

Considering batteries of 400 Ah at 12 V, the number of batteries that must be connected in parallel can be calculated using Equation (7):

$$N_{P,batt} = \frac{C_{T,batt}}{C_{U,batt}} = \frac{2154\ Ah}{400\ Ah} = 5.385 \approx 6 \quad (7)$$

where:
$N_{P,batt}$ is the number of batteries connected in parallel
$C_{U,batt}$ is the capacity of a unit battery in Ampere hours

The number of batteries that must be connected in series can be calculated using Equation (8):

$$N_{S,batt} = \frac{V_{DC}}{V_{U,batt}} = \frac{48}{12} = 4 \quad (8)$$

where:
$N_{S,batt}$ is the number of batteries connected in series
$V_{U,batt}$ is the unit voltage of the battery selected

The number of battery units required to meet the energy demand was determined using Equation (9):

$$N_{batt} = N_{P,batt} \times N_{S,batt} = 6 \times 4 = 24 \quad (9)$$

where:
$N_{P,batt}$ is the number of batteries connected in parallel
$N_{batt}$ is the total number of batteries required

The battery bank requires a 4-series, 6-parallel (4S6P) configuration using 24 batteries to achieve a total capacity of 2154 Ah at 48 V. A three-day (72 h) autonomy period for a household off-grid or backup solar system balances cost and reliability.

### 3.4.4. Inverter Sizing

PV modules generate power in the form of DC. To convert this DC electricity into AC electricity, an inverter system is required. Inverters are sized based on the power rating of AC loads, and their capacity must exceed the peak power demands of the loads. The inverter size can be determined using Equation (10).

$$I_S = D_{P,load} \times 1.25 = 1318 \times 1.25 = 1647.5 \approx 1648\ W \quad (10)$$

where:
$I_S$ is the required inverter capacity
$D_{P,load}$ is the daily peak load

The value of 1.25 represents the safety factor

To account for the appliance startup currents, transient loads, and potential future load growth, the inverter was oversized by 25%.

$$\text{The new inverter requirement} = 1648 \times 1.25 = 2060\ \text{W}$$

Consequently, a 2.06 kW, 48 V inverter was deemed suitable for the system.

Surge Capability Verification

- Inverter Capacity: The selected inverter, rated at 2.06 kW (2060 W), consistently delivers 2060 W and can handle a peak surge of 4200 W (4.2 kW) for short durations.
- Simultaneous Worst-Case Surge: In the event that both the refrigerator and freezer attempt to start at the exact same microsecond, the combined peak demand is 1800 W (900 W each).
- Staggered Operation: When one appliance is operational and the other commences, the combined peak demand is 1200 W, consisting of 300 W for running and 900 W for starting. This peak remained well below the inverter's continuous capacity of 2060 W.
- Safety Margin: The total simultaneous startup demand of 1800 W represented only 43% of the inverter's maximum surge capacity of 4200 W, thus maintaining a safe buffer of 2400 W to prevent low voltage trips or overloads.

### *3.5. Sizing Procedure Based on Supply Reliability*

This study aimed to optimize the sizing of components within a PV-battery system by formulating equations that calculate the generation adequacy. These equations incorporate a reliability index to measure system reliability. One method for evaluating supply reliability is the LPSP.

In this study, equations sourced from the literature [31] were utilized to develop a program capable of calculating the total energy generated by a PV array and determining the requisite number of batteries to achieve a specified LPSP. The battery charge efficiency was equated to the round-trip efficiency, and the discharge efficiency was set to 1. The inverter was rated according to the peak load demand, and a constant inverter efficiency was applied to reflect the average load demand.

The total available energy generated $E_G(t)$ by the PV array can be expressed as follows (Equation (11)):

$$E_G(t) = \left(N_{PV} \times E_{PV}(t)\right) \tag{11}$$

Here, $N_{PV}$ represents the number of PV modules in a PV array, and $E_{PV}(t)$ denotes the energy generated by a PV module (kWh).

The generated power is subject to the following constraint expressed in Equation (12):

$$E_G(t) \geq \frac{E_L(t)}{(\eta_{inv} \times \eta_{bat})} \tag{12}$$

Given that the battery charge efficiency is equated to the round-trip efficiency and the discharge efficiency is set to 1, two scenarios were considered to determine the energy stored in the batteries at time, *t*.

1. The batteries are charged with round-trip efficiency only when the energy generated from power sources, such as the PV array, exceeds the load demand. This scenario can be represented as follows (Equation (13)):

$$E_B(t) = E_B(t-1) \cdot (1-\sigma) + \left(E_G(t) - \frac{E_L(t)}{\eta_{inv}}\right) \cdot \eta_{batt,inv} \tag{13}$$

2. Conversely, when the load demand surpasses the energy generated by the PV array, the batteries discharge the necessary amount to compensate for any deficits. This scenario can be represented as follows (Equation (14)):

$$E_B(t) = E_B(t-1) \cdot (1-\sigma) - \left( \frac{E_L(t)}{\eta_{inv}} - E_G(t) \right) \quad (14)$$

Here $E_B(t)$ denotes the energy stored in the batteries at hour t (kWh), and $E_B(t-1)$ represents the energy stored in the previous hour (kWh), σ signifies the hourly self-discharge rate of the battery bank, $E_L(t)$ indicates the load demand during hour t (kW), $\eta_{inv}$ refers to the inverter efficiency, and $\eta_{batt,inv}$ denotes the round-trip efficiency of the batteries.

The energy stored in the batteries at any given hour *t* must adhere to the following constraint (Equation (15)):

$$E_{Bmin} \leq E_B(t) \leq E_{Bmax} \quad (15)$$

$E_{Bmin}$ represents the minimum allowable energy of the battery (Wh), and $E_{Bmax}$ denotes the maximum allowable energy of the battery (Wh).

When the energy generated and stored in the batteries is inadequate to satisfy the load demand at time *t*, the resulting deficit is termed the loss of power supply at time *t* and is expressed as follows (Equation (16)):

$$LPS(t) = E_L(t) - (E_G(t) + E_B(t-1) - E_{Bmin}) \cdot \eta_{inv} \quad (16)$$

In an ideal system in which the supply consistently meets the load, LPS(t) is zero. Conversely, in a system in which the load is never satisfied, LPS(t) equals a non-zero value. In this system-sizing program, the target LPS(t) was set to zero.

The LPSP for a given period T is calculated as the ratio of the sum of all LPS values at specific times (t) to the sum of the load demand $E_L(t)$ at the same times (t). This relationship is mathematically expressed as follows (Equation (17)):

$$LPSP = \frac{\sum LPS(t)}{\sum E_L(t)} \text{ (for } t \leq T) \quad (17)$$

The corresponding flowchart is presented in Figure 4.

This program was used to simulate the operation of a PV/battery system by conducting energy balance calculations for each hour over the course of a year. For each hour, the program evaluates the power generated in response to the electric load demand. It concurrently determines the charging and discharging strategies for the batteries. The logic used in this program was structured to adhere to the probability of loss of power supply. The LPSP calculation was performed in the MATLAB environment, and the results indicated that the system exhibited an LPSP of 0.0048%.

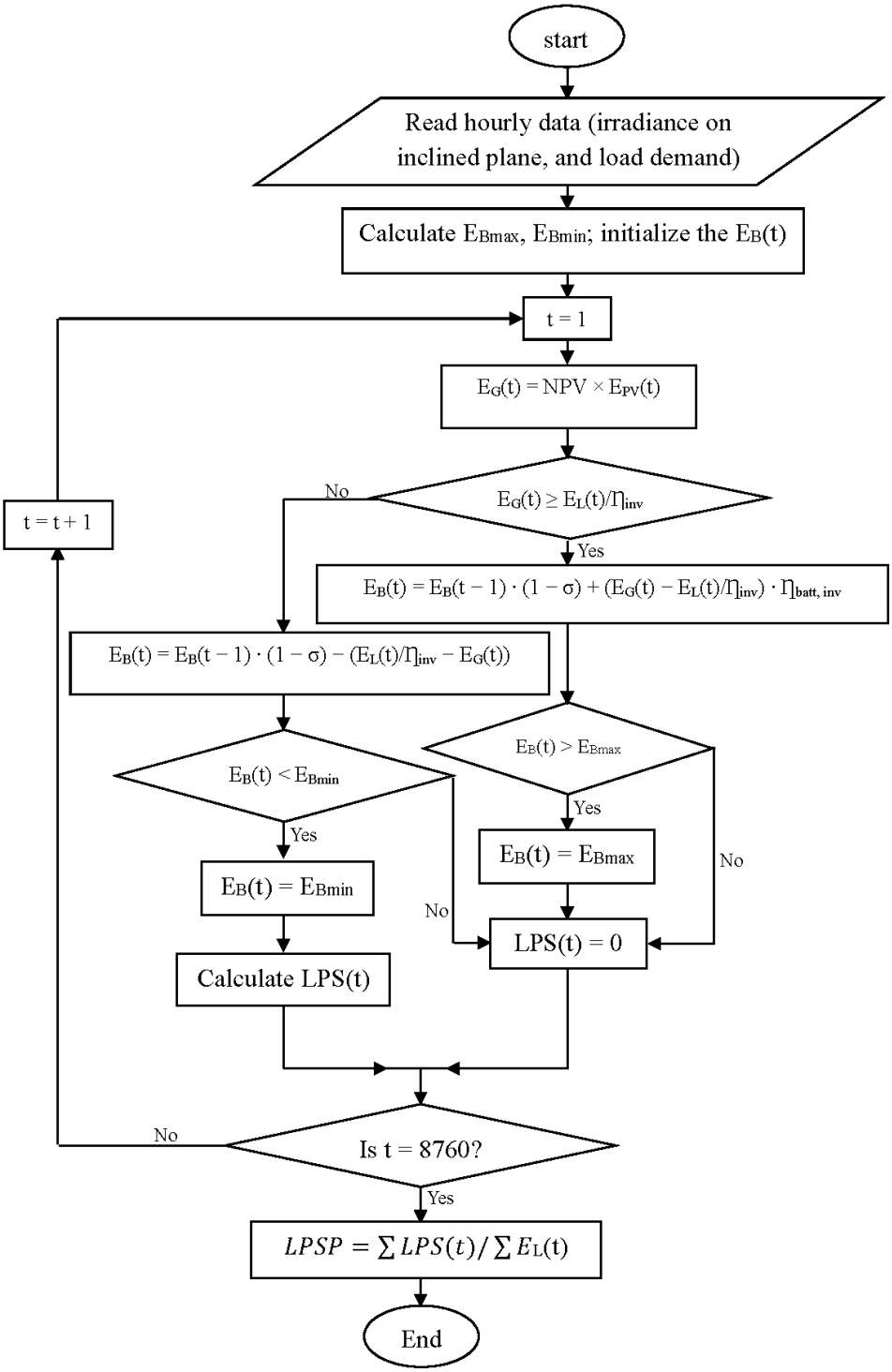



**Figure 4.** Flowchart for calculating the reliability of the power supply to the load.

### *3.6. Description of How HOMER Software Models Uncertainty in Load and Solar Resource*

HOMER software facilitates the simulation of off-grid SPV systems by balancing hourly solar energy production, battery storage, and load requirements over an annual period to ascertain the most cost-effective configuration. In HOMER Pro, a stochastic approach is employed, which utilizes time-series data to model the inherent uncertainty and variability of solar resources and load demands [32]. This software incorporates stochastic parameters to simulate the variability of load and solar resources by utilizing autoregressive moving average (Graham algorithm) and normal (Gaussian) distribution algorithms. Specifically, in its synthetic approach, HOMER uses the Graham algorithm to generate an 8760-h dataset

that mirrors the autocorrelation of actual measured data, while the Gaussian probability distribution is applied to introduce day-to-day and time-step randomness to user-defined base profiles [33]. Consequently, HOMER uses user-defined percentages applied as noise to the baseline data to perform stochastic simulations. These percentages, input into the software, represent the standard deviations (time-step-to-time-step and day-to-day variability), which HOMER uses to stochastically generate values during sequential calculations, primarily to model real-world uncertainties in solar resources and electrical loads.

To address solar resource variability, HOMER applies the Graham algorithm to generate synthetic hourly solar data from monthly average input. This approach ensures that cloudy hours follow each other, thereby mimicking real-world weather patterns [34]. For load variability, HOMER incorporates a Gaussian probability distribution to introduce a stochastic noise component, accounting for both time-step-to-time-step and day-to-day variability in synthetic daily load profiles, thus rendering the aggregate demand realistic. For aggregate rural residential or commercial loads, it is necessary to set the day-to-day and time-step load variability between 10% and 20% [35].

### 3.6.1. Simulation-Based Design of SPV System Using HOMER Software

A simple model was developed using HOMER software to design and simulate an SPV system. This model facilitates the simulation of an off-grid SPV system aimed at providing sustainable energy to households. Meteorological inputs, including latitude and longitude, were obtained from a field study of the household's geographical location, as shown in Figure 5. The primary load profile was configured to operate continuously for 24 h a day throughout the year, as detailed in Appendix A, which contains household load consumption data. The costs of key components, such as hardware, installation, and labour, as well as the interest and inflation rates for capital investments, were based on actual local market prices, as indicated in Appendix B. Data for each component, including capacity, search range, and costs (capital, replacement, and operation and maintenance), as outlined in Table 5, were input into the software. The optimization settings and economic assumptions are presented in Table 6.




**Figure 5.** Solar radiation throughout the year.

**Table 5.** Component capacity, search ranges, and costs used in the simulation.

| Component | Capacity | Search Range | | ** Capital Cost | ** Replacement Cost | O & M Cost |
|---|---|---|---|---|---|---|
| | | Lower | Upper | | | |
| PV | 0.415 kW | 0 | 11 | ₦140,000.00 | ₦135,500.00 | ₦1000.00 |
| Battery | 400 Ah, 12 V | 0 | 9 | ₦400,000.00 | ₦390,000.00 | ₦1000.00 |
| Converter | 1 kW | 0 | 4 | ₦38,900.00 | ₦38,900.00 | ₦100.00 |

** [36,37].

**Table 6.** Optimization settings and economic assumptions.

| | |
|---|---|
| Discount rate (%) | 26.50 |
| Inflation rate (%) | 15.90 |
| Project lifetime (year) | 25.00 |
| Minutes per time-step | 60 |
| Annual capacity shortage (%) | 0.00 |
| Load in current time-step (%) | 20 |
| Random variability: Day-to-day (%) | 10 |
| Random variability: Time-step (%) | 20 |
| PV derating factor (%) | 90.00 |
| Converter Efficiency (%) | 95.00 |
| Battery Minimum State of Charge (%) | 20.00 |
| Controller Dispatch Strategy | Load-following |

### 3.6.2. Stochastic Procedure

This PV/battery system was designed to fulfill the energy requirements of rural residential areas by incorporating real-world environmental and behavioural uncertainties. Traditional deterministic models frequently underestimate the reliability of renewable sources due to their reliance on static average values. To overcome this limitation, the present study employed the HOMER optimization model to conduct chronological time-series simulations that incorporate robust stochastic procedures. In this context, the stochastic procedure refers to the method by which the HOMER software introduces and manages randomness in real-world variables during chronological simulations. To simulate realistic environmental volatility, the HOMER model applied the Graham algorithm to synthetic hourly solar data derived from monthly averages. This method preserves temporal autocorrelation, ensuring that consecutive cloudy hours accurately reflect natural weather persistence. Concurrently, human behavioural unpredictability and demand fluctuations were modeled by incorporating a Gaussian probability distribution into the load profiles. Stochastic noise parameters were configured with a 10% time-step and a 20% day-to-day standard deviation, thereby establishing a realistic aggregate demand profile that effectively captures both micro-level appliance cycling and macro-level daily behavioural shifts. The incorporation of these variability percentages into the synthetic daily load profile led to modifications in the peak load, which increased from 1.32 to 2.25, and in the load factor, which decreased from 0.66 to 0.39, as illustrated in Figures 6 and 7. The application of these integrated probabilistic distributions in the simulation effectively prevented the underestimation of peak demands and accounted for the inherent uncertainties associated with solar energy generation. The resulting 8760-h time-series data were exported and systematically analyzed in a spreadsheet to assess critical performance metrics, including true coincident peak demands, system capacity shortages, and battery throughput. This stochastic framework ultimately ensures that the proposed PV/battery system is appropriately sized, resilient to volatile load spikes, and optimized for long-term operational reliability.

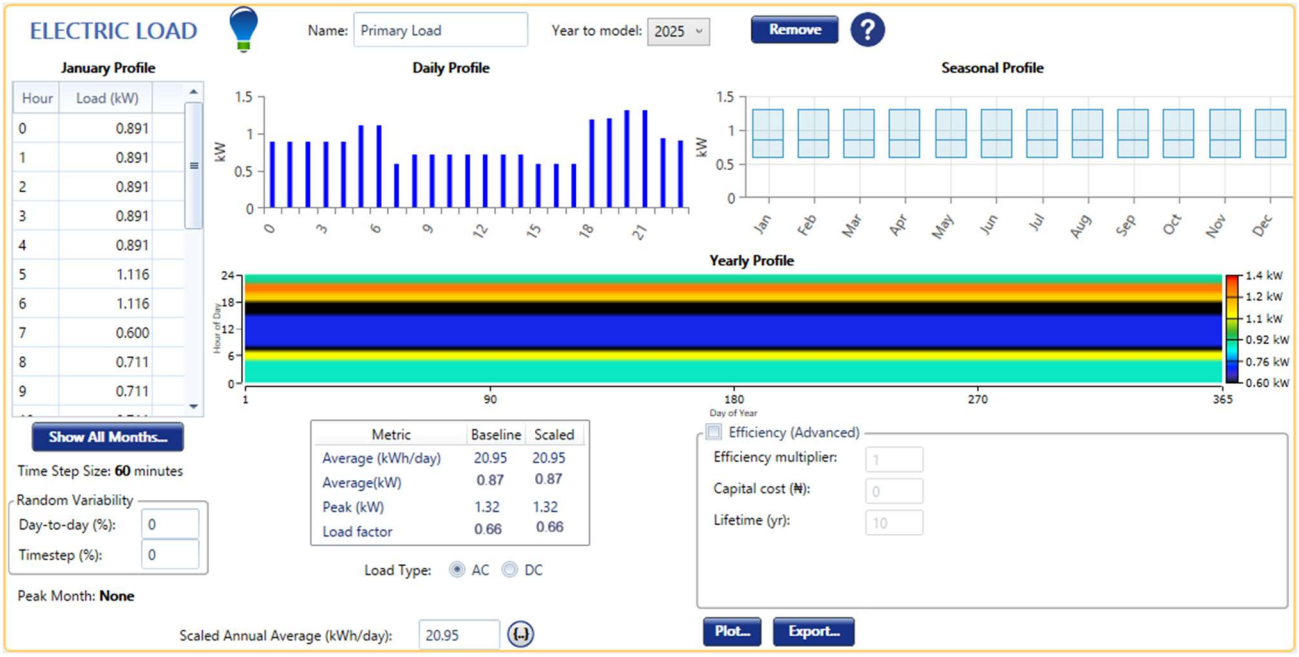



**Figure 6.** Screenshot of electricity load demand for baseline data with 0% daily noise and 0% hourly noise.

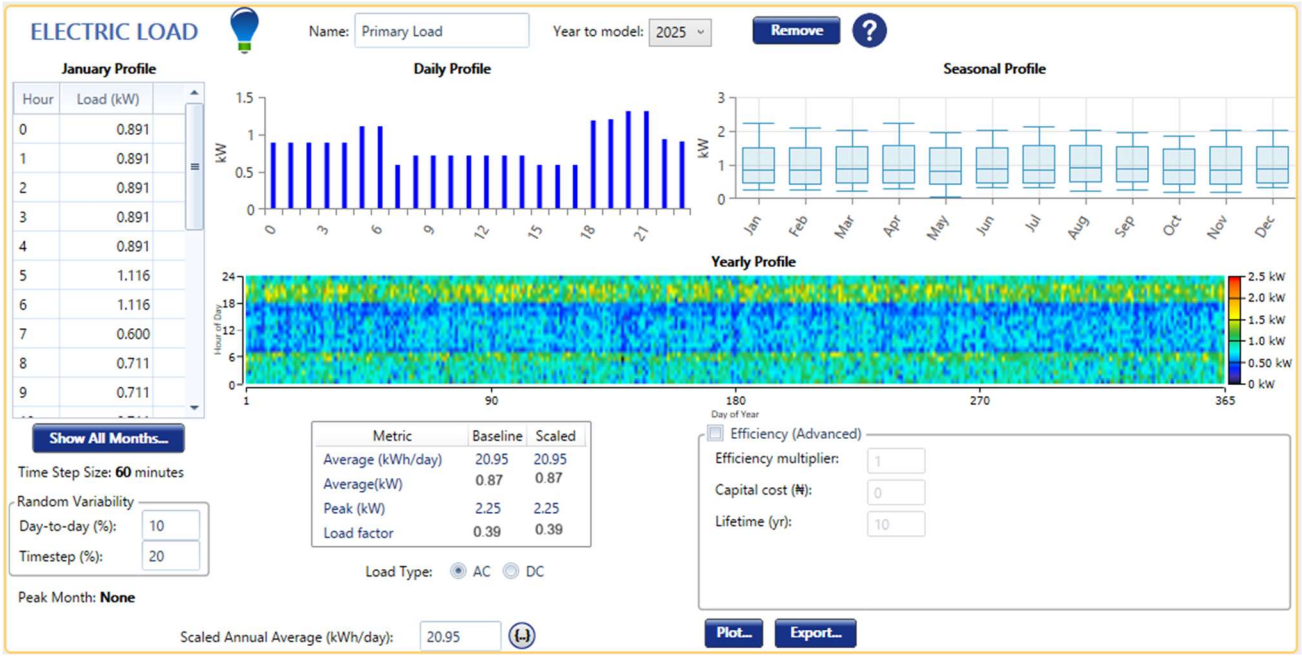



**Figure 7.** Screenshot of electricity load demand for baseline data with 10% daily noise and 20% hourly noise.

In HOMER, water pumping is classified as a deferrable load, which is defined as an electrical load associated with storage that requires a specific amount of energy to operate within a designated time frame. To accurately model this scenario in HOMER, the following parameters were input into the model (Figure 8):

1. The daily pumping load was 2.19 kWh.
2. The energy required to fill the tank was 4.27 kWh.
3. The peak load of the pump was 1.09 kW.
4. The minimum power required to sustain the pump load was 22.94%.




**Figure 8.** Water pumping in HOMER: Deferrable load.

The system architecture, depicted in Figure 9 and elaborated in Appendix C (Figures A1–A9), consists of a load-following controller, 24-unit 400 Ah batteries, 2.29 kW inverter, and 8.86 kW PV array.

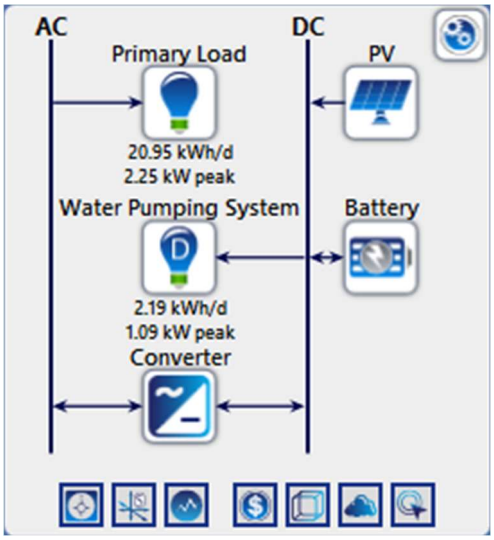



**Figure 9.** Schematic of the designed off-grid SPV system.

Furthermore, a simulation of the diesel-battery system was conducted to facilitate a comparative analysis with the PV-battery system.

### 3.6.3. Load Profile Justification and HOMER Simulation Reproducibility

To develop the proposed standalone off-grid system, a bottom-up mathematical synthesis method was employed to generate an hourly load profile. This profile for household energy use was derived from a comprehensive list of typical domestic appliances, including their power ratings (W), daily usage periods, and an estimated coincidence factor. To reflect the randomness of human behaviour and the unpredictable patterns of residential energy use, parameters for synthetic variability were incorporated daily and at each timestep. This methodology ensures that the simulated power system experiences realistic operational

challenges, with transient peak demands that accurately determine the required surge capacities for the inverter and battery bank.

To guarantee the precise reproducibility of the optimization outcomes, a synthetic load profile was integrated into HOMER Pro (version 3.18.4) using fixed random seeds and specific variability constraints. The baseline profile created had an average daily consumption of 20.95 kWh/day and a peak load of 2.25 kW, resulting in a load factor of 0.39. Within the 8760-h simulation, stochastic variation was limited by setting day-to-day variability at 10% and timestep-to-timestep variability at 20%. The search space for the standalone system optimization was conducted using the HOMER Optimizer. Operating constraints were strictly adhered to, with a maximum annual capacity shortage of 0.00% and a minimum battery state-of-charge (SoC) of 20%, which is typical for 12 V 400 Ah Li-ion chemistry. Renewable resource data were aligned chronologically using the NASA Prediction of Worldwide Energy Resources (POWER) database for a specific coordinate profile.

## 4. Results and Discussions

### *4.1. Technical Analysis*

Tables 7 and 8 present comprehensive data on the system components and electrical output, respectively, for the comparative study. The PV/battery system produced 5278 kWh of excess electricity annually. This surplus was due to the inclusion of stochastic variability in the model, which increased the peak demand. Furthermore, stochastic variability provides a more precise assessment of battery life and SPV system efficiency by necessitating simulations to manage fluctuating solar energy output and unpredictable loads.

**Table 7.** Simulation Details of the PV System Compared with Diesel System Components.

| Quantity | PV/Battery System | | | Diesel/Battery System | | | |
|---|---|---|---|---|---|---|---|
| | PV | Inverter | Battery | Diesel | Inverter | Rectifier | Battery |
| Capacity (kW) | 8.86 | 2.29 | ** 400 | 2.70 | 2.17 | 2.17 | ** 400 |
| Mean Output (kW) | 1.64 | 0.873 | | 2.70 | 0.491 | 0.629 | |
| Capacity Factor (%) | 18.5 | 38.1 | | 38.7 | 22.7 | 29.0 | |
| Hours of Operation (h/yr.) | 4380 | 8759 | | 3389 | 5372 | 3388 | |
| Number of Starts (Starts/yr) | | | | 466 | | | |
| Fuel Consumption (L) | | | | 2670 | | | |
| Operational Life (yr.) | 25.0 | 15.0 | 15.0 | 4.43 | | | 4.43 |
| Number of Batteries (Qty.) | | | 24.0 | | | | 4.00 |
| Batteries in Series (Qty.) | | | 4.00 | | | | 4.00 |
| Batteries in Parallel (Qty.) | | | 6.00 | | | | 1.00 |
| Nominal Voltage (V) | | | 48.0 | | | | 48.0 |
| Autonomy (h) | | | 95.6 | | | | 15.9 |
| Usable Capacity (kWh) | | | 92.2 | | | | 15.4 |
| Energy In (kWh/yr.) | | 8047 | 5371 | | 4531 | 5803 | 4715 |
| Energy Out (kWh/yr.) | | 7645 | 5165 | | 4304 | 5513 | 4532 |
| Losses (kWh/yr.) | | 402 | 215 | | 227 | 290 | 189 |
| Annual Throughput (kWh/yr.) | | | 5271 | | | | 4625 |
| Lifetime Throughput (kWh) | | | 79,067 | | | | 20,480 |

** The battery capacity value of 400 Ah is for the single battery.

**Table 8.** Simulation details of electrical production and consumption.

| Quantity | PV System | | Diesel System | |
|---|---|---|---|---|
| | kWh/yr | % | kWh/yr | % |
| AC Primary Load | 7645 | 90.6 | 7647 | 90.5 |
| Deferrable Load | 798 | 9.40 | 798 | 9.5 |
| Total Load Met | 8443 | 100 | 8445 | 100 |
| Renewable Fraction | | 100 | | 0 |
| Energy Production | 14,329 | | 9146 | |
| Excess Electricity | 5278 | 36.8 | 0 | 0 |
| Unmet Load | 2.15 | 0.0255 | 0 | 0 |
| Capacity Shortage | 8.19 | 0.0970 | 0 | 0 |

#### 4.1.1. Sensitivity Analysis on the Effect of Changes in Solar Irradiance and Load Growth on System Performance and Economics

A comprehensive sensitivity analysis involving multiple variables was performed to assess the robustness and reliability of the technical evaluations and examine the financial profile of the project. By systematically comparing three levels of solar irradiance with three levels of load growth, a matrix of nine operational scenarios was developed. This approach with multiple variables illustrates how variations in external factors lead to physical changes in system size and affect the lifecycle costs. The results of the sensitivity analysis, as presented in Table 9, indicate that an increase in solar irradiance from a baseline of 4.93 kWh/m$^2$/d to 5.93 kWh/m$^2$/d, while maintaining a constant load of 21.0 kWh/d, leads HOMER to reduce the PV array size by 1.55 Kw due to the enhanced yield per panel. Notably, the battery bank remained unchanged at 24 units, suggesting that this number is the optimal threshold necessary to support nighttime loads for a demand of 21 kWh/day, irrespective of the daytime surplus. The inverter size experienced a slight increase from 2.29 kW to 2.52 kW. Although the total PV capacity was reduced, the peak hourly power demands resulting from the higher solar irradiance of 5.93 kWh/m$^2$/d necessitated a marginally larger inverter to accommodate the increased daytime power without causing bottlenecks. As each panel produced more power, the system reduced its PV capacity, thereby lowering the initial capital expenditure. This adjustment resulted in a 3.3% decrease in the total NPC, a 3.6% reduction in the LCOE, and a 1.29% decrease in annual operating costs. The unmet load increased marginally from 2.15 to 3.21 kWh per year. Given a total annual load of 7665 kWh, a 3.21 kWh shortfall is statistically negligible, ensuring the system achieves a 99.96% reliability rate. Clipped energy decreased by 5.7% (from 5278 to 4975 kWh per year), despite the more intense solar resource, indicating a highly optimized system. The reduction in the PV array size resulted in less excess power being wasted.

Reducing solar irradiance (SI) by 20% from 4.93 to 3.93 kWh/m$^2$/d, while maintaining a constant daily load of 21 kWh/d, necessitated a substantial increase in system hardware to satisfy demand, thereby elevating both capital and operational expenditure. HOMER incorporated an additional 1.54 kW of PV modules, four battery units, and an enlarged 2.51 kW inverter to ensure that the system could meet the 21 kWh/d load requirement under suboptimal weather conditions. The system experienced reduced energy wastage due to diminished peak sunlight, which limited the excess energy that could not be stored in the batteries. The unmet load increased from 2.15 to 4.67 kWh/yr, indicating a slight decline in system reliability. Consequently, the requirement for larger components resulted in a 17% increase in the NPC, a 16.8% increase in the LCOE, and a 16.7% increase in the operating costs.

With an increase in LG of 4.8% (from 21.0 to 22.0 kWh/d) while maintaining a constant solar irradiance of 4.93 kWh/m$^2$/d, the HOMER model opted to incorporate an additional 0.68 kW of PV capacity and significantly enlarge the inverter to 2.67 kW, representing a 16.6% increase. This adjustment enabled the system to harness and process a greater amount of peak daytime power to meet the elevated demand

directly. Notably, the battery bank remained unchanged at 24 units, suggesting that the existing battery storage capacity was sufficiently robust to accommodate the overnight segment of the additional 1 kWh/d demand, assuming adequate daytime solar generation to maintain the charge. The clipped energy experienced a 13.4% increase, which is a consequence of oversizing the solar array; during peak sunlight hours, when the 24 batteries are fully charged, the expanded 9.54 kW array resulted in a higher amount of unused power. Consequently, unmet load increased to 4.67 kWh/yr. With a total annual load of 8030 kWh (22 kWh/d × 365), this reflects an exceptionally high reliability rate of 99.94%. This optimization strategy resulted in a 2.0% increase in the NPC but achieved a 2.5% reduction in the LCOE due to better utilization of the generated solar power.

Reducing LG by 4.8% (from 21.0 to 20.0 kWh/d) while maintaining a constant solar irradiance of 4.93 kWh/m$^2$/d leads HOMER to increase the PV capacity by 1.1 kW and expand the inverter by 0.28 kW, while significantly decreasing the system's battery storage by four units. This structural adjustment results in a 10.5% reduction in the NPC but a 6.4% increase in the LCOE, primarily due to a substantial increase in energy wastage (clipped energy). This unexpected outcome exemplifies one of the intriguing behaviours of the HOMER Pro optimization engine. The engine determines that it is more economically advantageous to overproduce energy during the day, leading to a substantial 40.4% increase in clipped energy (7411 kWh/yr) and discard it rather than incur the cost of storing it. HOMER determined that for a slightly reduced load of 20 kWh/d, it is more cost-effective to significantly reduce the battery bank from 24 to 20 units. Considering the high cost of batteries, this adjustment results in substantial capital savings. To compensate for the reduced storage capacity during nighttime, HOMER incorporates an additional 1.07 kw of PV capacity to directly power the load during the day and expedite the charging of the smaller battery bank. Due to the PV array being oversized by 12.1% and the battery storage being downsized by 16.7%, the system experiences a significant 40.4% increase in clipped energy. Consequently, the system often generates more daytime power than the smaller battery bank can accommodate, resulting in 7411 kWh/yr of discarded electricity. The unmet load more than doubled to 5.46 kWh per year, indicating a slight compromise in system reliability in favour of substantial capital savings. Despite this, the system maintains an impressive reliability rate of 99.93% out of an annual demand of 7300 kWh (calculated as 20 kWh per day × 365 days). The energy cost decreased to 174.91 ₦/kWh attributed to the significant reduction in battery capital expenditure. However, the substantial amount of clipped energy affects the economic efficiency per kilowatt-hour actually utilized.

When solar irradiance decreased while the load increased, it led to a rise in the PV array capacity to 10.5 kW and the addition of 32 battery units, resulting in the highest LCOE of ₦233.13/kWh and a peak NPC of ₦19.9 million. Conversely, when the solar input increases and the load decreases, a smaller battery bank can be utilized. These results suggest that the system design approach can be modified for use in other parts of Nigeria or in developing countries with varying climatic conditions and load requirements.

**Table 9.** Results of the sensitivity analysis on the effect of changes in solar irradiance and load growth on system performance and economics.

| Sensitivity Analysis | Solar Irradiance [SI]—(kWh/m$^2$/d) | Load Growth [LG]—(kWh/d) | PV 415 (kW) | Battery (Units) | Inverter (kW) | Capacity Shortage (kWh/yr) | Clipped Energy (kWh/yr) | Unmet Load (kWh/yr) | Total NPC (Million ₦) | LCOE (₦/kWh) | Operating Cost (₦/yr) |
|---|---|---|---|---|---|---|---|---|---|---|---|
| Baseline | 4.93 | 21.0 | 8.86 | 24 | 2.29 | 8.19 | 5278 | 2.15 | 15.3 | 186.81 | 271,110 |
| SI Lowered | 3.93 | 21.0 | 10.4 | 28 | 2.51 | 8.09 | 4366 | 4.67 | 17.9 | 218.22 | 316,305 |
| SI Increased | 5.93 | 21.0 | 7.31 | 24 | 2.52 | 8.29 | 4975 | 3.21 | 14.8 | 180.15 | 267,612 |
| SI and LG Lowered | 3.93 | 20.0 | 10.3 | 24 | 2.93 | 7.97 | 4614 | 4.41 | 15.9 | 202.30 | 275,220 |
| LG Lowered | 4.93 | 20.0 | 9.93 | 20 | 2.57 | 8.06 | 7411 | 5.46 | 13.7 | 174.91 | 232,740 |

| | | | | | | | | | | | |
|---|---|---|---|---|---|---|---|---|---|---|---|
| SI Increased and LG Lowered | 5.93 | 20.0 | 8.27 | 20 | 2.46 | 8.04 | 7221 | 5.36 | 13.1 | 167.22 | 228,641 |
| SI Lowered and LG Increased | 3.93 | 22.0 | 10.5 | 32 | 2.63 | 8.48 | 4120 | 4.91 | 19.9 | 233.13 | 357,931 |
| LG Increased | 4.93 | 22.0 | 9.54 | 24 | 2.67 | 8.76 | 5984 | 4.67 | 15.6 | 182.19 | 273,131 |
| LG and SI Increased | 5.93 | 22.0 | 7.95 | 24 | 2.51 | 8.55 | 5801 | 4.34 | 15.0 | 175.38 | 269,131 |

#### 4.1.2. Sensitivity Analysis of the Impact of Component Efficiency Variations on System Performance and Economics

An extensive sensitivity analysis was performed to assess how changes in PV derating factors (ranging from 85.0% to 95.0%) and inverter efficiencies (spanning 90.0% to 98.0%) affect both the technical and economic aspects of the baseline system configuration. The baseline setup, featuring a PV derating factor of 90.0% and an inverter efficiency of 95.0%, yielded a total NPC of ₦15.3M, LCOE of ₦186.81/kWh, and an annual operating cost of ₦271,110, supported by an 8.86 kW PV array and a battery bank consisting of 24 units. The results of the sensitivity analysis are presented in Table 10.

Decreasing the PV derating factor while maintaining the inverter efficiency at a constant 95% necessitated the expansion of the system's generation and conversion capacities. Consequently, the PV array size increased from 8.86 kW to 9.32 kW, and the inverter capacity significantly increased from 2.29 kW to 3.03 kW to accommodate the adjusted peak outputs. The battery storage was constant at 24 units. Despite the enlarged PV and inverter configuration, the unmet load experienced a slight increase from 0.0255% to 0.0369%. Nevertheless, the increased inverter capacity effectively reduced clipped energy marginally, from 36.8% to 36.4%, and enhanced the overall capacity shortage risks. This expanded system architecture led to increases in all financial metrics. The total NPC increased by ₦200,000, rising from ₦15.3 million to ₦15.5 million, whereas the LCOE increased by ₦2.48/kWh, from ₦186.81 to ₦189.29. Additionally, annual operating costs experienced a slight increase of ₦1864.

By increasing the PV derating factor from 90% to 95% while maintaining the inverter efficiency at its baseline value of 95.0%, HOMER Pro effectively reduced the PV array size by 5.87%, decreasing from 8.86 kW to 8.34 kW, while continuing to satisfy the primary load requirements. Although the total installed PV capacity was reduced, the enhanced efficiency resulted in a greater peak DC output during peak sunlight hours. To accommodate this concentrated energy without excessive throttling, HOMER increased the inverter capacity by 10.04%, from 2.29 kW to 2.52 kW. This modification decreased the clipped energy from 36.8% to 36.4%. The battery count was constant at 24 units. The capacity shortage remained nearly unchanged at 0.0969%, although the system accepted a slight increase in unmet load to 0.0369% to achieve overall hardware cost reductions. Improved panel performance resulted in a reduction in overall project costs, with the NPC decreasing by ₦200,000 to ₦15.1 million and the LCOE decreasing by ₦2.14 per kWh, from ₦186.81 to ₦184.67. The annual operating costs also showed a minor decline of ₦1022.

Reducing the inverter efficiency from 95.0% to 90.0% while maintaining the PV derating factor at its baseline value of 90.0% results in a 5% increase in energy loss during the DC-to-AC conversion process. To compensate, HOMER Pro expands the PV array by 8.92%, increasing its capacity from 8.86 kW to 9.65 kW, to supply more power to the system. Consequently, the inverter capacity is scaled up by 14.41%, reaching 2.62 kW, to accommodate the larger PV volume. However, due to the reduced efficiency of the inverter, a substantial portion of this energy cannot be safely or efficiently converted, leading to an increase in clipped energy to 39.1%. The battery bank remained constant at 24 units. Although the risk of capacity shortage decreased slightly to 0.0945%, the system's actual delivery performance declined significantly, with the unmet load more than doubling from 0.0255% to 0.0550%. The necessity for larger hardware increases all

financial metrics. The total NPC rose by ₦300,000, reaching ₦15.6 million, while the LCOE increased by ₦3.74 per kWh, from ₦186.81 to ₦190.55. Additionally, operating costs escalated by ₦2251 annually.

Enhancing the inverter efficiency from 95.0% to 98.0%, while maintaining the PV derating factor at a constant baseline of 90.0%, resulted in significant system improvement. The inverter's ability to recover 3% of the power previously lost as heat during the DC-to-AC conversion process allowed HOMER Pro optimization to reduce the required PV array size by 4.63%, from 8.86 kW to 8.45 kW. The inverter capacity was incrementally increased to 2.37 kW, a 3.49% increase, to effectively manage the enhanced energy throughput. This optimization, coupled with a reduced solar size, substantially decreased power wastage, lowering the clipped energy by 35.6%, with a total reduction of 1.2%. The structural integrity of the system was preserved using 24 battery units. The capacity shortage experienced a slight decrease to 0.0962%, while the unmet load marginally increased from 0.0255% to 0.0287%, representing a negligible compromise for the hardware efficiency gains. The NPC decreased by ₦100,000, falling to ₦15.2 million, and the LCOE decreased by ₦1.75/kWh, reaching ₦185.06/kWh. The annual operating costs also decreased by ₦900.

When the PV derating factor increased to 95.0%, indicating minimal environmental losses, and the inverter efficiency reached 98.0%, HOMER adjusted the storage architecture by reducing the battery bank from 24 to 20 units. Due to the high efficiency of generation and conversion, the system became less dependent on substantial chemical storage for energy delivery stabilization. With reduced storage costs, HOMER rebalanced the PV/battery system towards active generation, resulting in a 10.84% expansion of the PV array to 9.82 kW and an increase in inverter capacity to 2.72 kW. The reduction in the battery units led to significant life-cycle savings. The total NPC decreased by ₦1.6 million, reaching ₦13.7 million, while the LCOE declined by 10.63% to ₦166.95 per kWh. Additionally, the annual operating costs were reduced by ₦38,477. To realize these substantial financial savings, the system design accommodated increased volatility. The proportion of clipped energy increased to 47.6% due to the substantial output of the solar array, and the unmet load increased to 0.0676% due to a slightly reduced battery bank capacity.

Two behaviours were observed: first, increased PVD and IE led to the use of smaller batteries but larger PV arrays, and second, increased PVD alone necessitated larger inverters. These unexpected optimization outcomes often occur because the software identifies cost-effective combinations within specific search spaces, focusing on minimizing total NPC rather than strictly following linear physical scaling.

In conclusion, the sensitivity analysis demonstrated that the economic and technical viability of the PV/battery system is highly sensitive to variations in PV derating and inverter efficiency. Concurrently optimizing both parameters yields the most cost-effective configuration while simultaneously optimizing the component size. However, when these efficiency metrics decline, the system is compelled to increase its PV and inverter capacities to offset performance reductions, leading to higher overall capital and annual operating costs. In the context of Nigeria's energy sector, these results have important implications for investments and policies. From a financial perspective, the project's baseline LCOE of 186.81 ₦/kWh remains competitive compared to the increasing operational costs of conventional diesel generation, which have worsened by the removal of fuel subsidies. However, specific policy measures are necessary to maintain the long-term commercial viability of developers. The Standard Organisation of Nigeria (SON) and the Nigerian Electricity Regulatory Commission (NERC) need to enforce stringent quality standards on imported solar components to avoid the use of substandard equipment that could significantly degrade system performance. Furthermore, the Federal Government should enhance fiscal incentives, such as duty exemptions for high-efficiency inverters and advanced battery technologies, to reduce the total upfront NPC. These strategies will reduce investment risks, accelerate capital recovery for private developers, and offer rural communities more cost-effective and sustainable PV/battery systems.

**Table 10.** Results of the sensitivity analysis on the effect of changes in component efficiencies on system performance and economics.

| Sensitivity Analysis | PV Derating [PVD] (%) | Inverter Efficiency [IE] (%) | PV 415 (kW) | Battery (Units) | Inverter (kW) | Capacity Shortage (%) | Clipped Energy (%) | Unmet Load (%) | Total NPC (Million ₦) | LCOE (₦/kWh) | Operating Cost (₦/yr) |
|---|---|---|---|---|---|---|---|---|---|---|---|
| Baseline | 90.0 | 95.0 | 8.86 | 24 | 2.29 | 0.0970 | 36.8 | 0.0255 | 15.3M | 186.81 | 271,110 |
| PVD Lowered | 85.0 | 95.0 | 9.32 | 24 | 3.03 | 0.0942 | 36.4 | 0.0369 | 15.5M | 189.29 | 272,974 |
| PVD Increased | 95.0 | 95.0 | 8.34 | 24 | 2.52 | 0.0969 | 36.4 | 0.0369 | 15.1M | 184.67 | 270,088 |
| PVD and IE Lowered | 85.0 | 90.0 | 10.2 | 24 | 2.55 | 0.0946 | 39.1 | 0.0549 | 15.8M | 193.01 | 274,657 |
| IE (declined) | 90.0 | 90.0 | 9.65 | 24 | 2.62 | 0.0945 | 39.1 | 0.0550 | 15.6M | 190.55 | 273,361 |
| PVD Increased and IE Lowered | 95.0 | 90.0 | 9.13 | 24 | 3.18 | 0.0995 | 39.0 | 0.0556 | 15.5M | 188.60 | 272,687 |
| PVD Lowered and IE Increased | 85.0 | 98.0 | 8.96 | 24 | 2.32 | 0.0963 | 35.7 | 0.0233 | 15.3M | 187.26 | 271,380 |
| IE Increased | 90.0 | 98.0 | 8.45 | 24 | 2.37 | 0.0962 | 35.6 | 0.0287 | 15.2M | 185.06 | 270,210 |
| PVD and IE Increased | 95.0 | 98.0 | 9.82 | 20 | 2.72 | 0.0999 | 47.6 | 0.0676 | 13.7M | 166.95 | 232,633 |

### *4.2. Comparison of Manual Calculations and Simulation*

The manually calculated LPSP was 0.0048%, whereas the simulation produced a result of 0.0255%. The manual calculations recommended a PV capacity of 8.47 kW, along with 24-unit 400 Ah batteries and a 2.06 kW inverter. In contrast, the simulation proposed a PV capacity of 8.86 kW, keeping the battery count unchanged but using a 2.29 kW inverter. It is noteworthy that the manually determined sizes for the PV system and inverter (8.47 kW and 2.06 kW, respectively) differed from those suggested by the HOMER simulation, which were 8.86 kW for the PV system and 2.29 kW for the inverter. This discrepancy is due to variations in peak load: manual calculations yielded 1.32 kW, while simulations showed 2.25 kW. This variation is attributed to the simulation's inclusion of a 10% standard deviation for daily noise and a 20% standard deviation for hourly noise, which requires larger inverter and PV system sizes. Moreover, the synthetic hourly solar data, based on the provided monthly averages, improved energy production, resulting in excess electricity generation.

### *4.3. Economic Cost of PV/Battery System*

The economic cost of the designed energy system comprises the calculated system operating cost, life cycle cost, and levelized cost of electricity. The simulation results showed that the levelized cost of electricity for the designed system was ₦186.81 Nigerian naira (NGN), which is the average cost per kWh of the electrical energy produced by the system.

#### 4.3.1. System's Operating Cost

The operating cost of an energy system is defined as the annualized value of all expenses and revenues, excluding the initial capital cost. From the simulation results shown in Figure 10, the operating cost was calculated as:

$$\text{Operating Cost} = \text{Total annualized cost} - \text{Capital annualized cost}$$
$$= ₦\,1{,}577{,}098.80 - ₦\,1{,}305{,}988.56 = ₦\,271{,}110.24$$

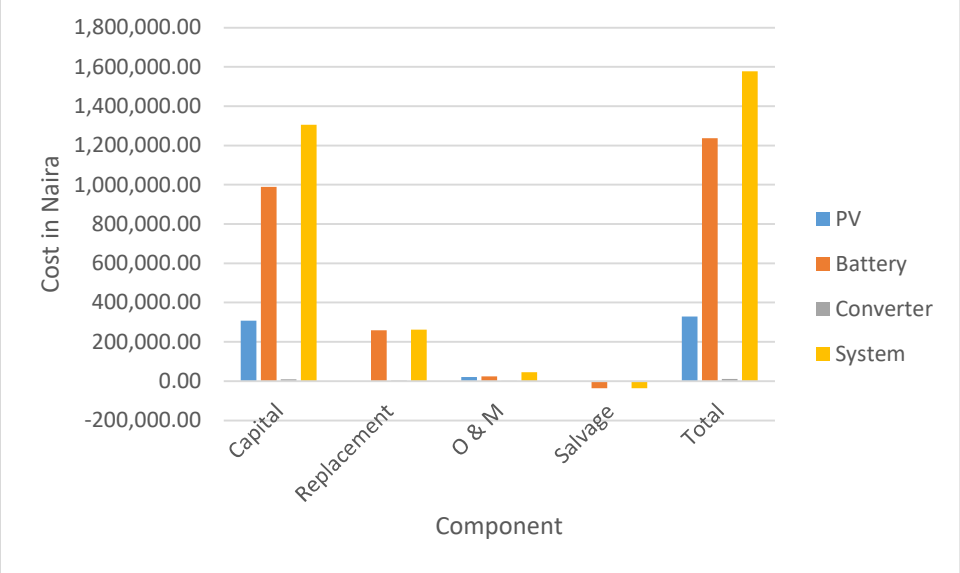



**Figure 10.** Annualized cost of the system.

### 4.3.2. System's Life-Cycle Cost

The life-cycle cost of an off-grid SPV system is the total expense incurred throughout its lifespan. This includes the initial capital investment, which covers the purchase and installation of PV modules, batteries, charge controllers, and inverters, as well as maintenance, battery and inverter replacement, and transportation costs [38]. According to HOMER, the life-cycle cost is defined as the present value of all expenses associated with installing and operating the system over its project lifetime, minus the present value of all revenues generated during the same period.

From the simulation results shown in Figure 11, the life cycle cost was calculated as:

$$\text{Life} - \text{Cycle Cost} = (\text{Capital} + \text{Replacement} + \text{O\&M}) - \text{Salvage}$$

$$= (₦\,12{,}678{,}082.55 + ₦\,2{,}542{,}638.32 + ₦\,442{,}463.91) - ₦\,353{,}258.35 = ₦\,15{,}309{,}926.43$$

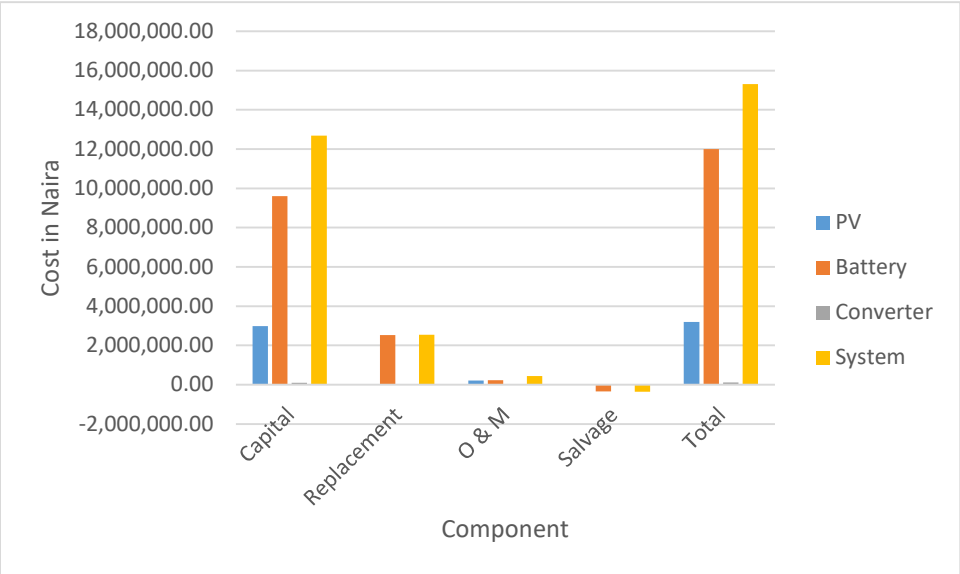



**Figure 11.** Net present cost (life cycle cost) of the system.

### *4.4. Compare Economics*

Figure 12 shows that the capital expenditure for the proposed solar PV/battery system was five times that of the conventional diesel/battery system. In terms of replacement costs, the diesel system required ₦4,067,373.80 for component replacements throughout its lifespan, which exceeded the cost of the PV system by ₦1.52 million, with the latter costing ₦2,542,638.32. This indicates that diesel generators undergo degradation and require overhauls or complete replacements more frequently than solar inverters and batteries. Regarding operations and maintenance (O&M) expenses, the PV system incurred routine O&M costs that were 3.7 times higher (₦442,463.91) than the diesel system (₦120,879.10). This disparity is typical because extensive solar/battery arrays require ongoing panel cleaning, thermal management, and electrical inspections. Moreover, the diesel system's O&M cost appeared deceptively low at ₦120,879.10, as significant mechanical overhauls were classified under "Replacement" costs rather than standard routine maintenance. However, the minor additional cost was completely eclipsed by the fuel savings. Fuel costs alone accounted for 88.92% of the total lifetime cost of the diesel system. The PV system offered a salvage value of ₦353,258.35, which exceeded the diesel system's residual asset value of ₦91,788.29 by ₦261,470.06. As depicted in Figure 13, the diesel system's operational costs were a staggering ₦51,951,907.18 (covering fuel and O&M), whereas the PV system's expenses were merely ₦442,463.91. Furthermore, the total NPC presented in Figure 13 indicates that the PV/battery system is significantly more cost-effective, delivering substantial lifecycle savings of ₦42,978,199.59 throughout the project duration compared with the diesel/battery system. This 25-year project featured an internal rate of return of 58% and a simple payback period of 1.7 years (*i.e.*, 20 months). The levelized cost of electricity for the designed PV/battery system was ₦186.81/kWh, whereas that of the diesel/battery system was ₦710.99/kWh, as shown in Figure 13.

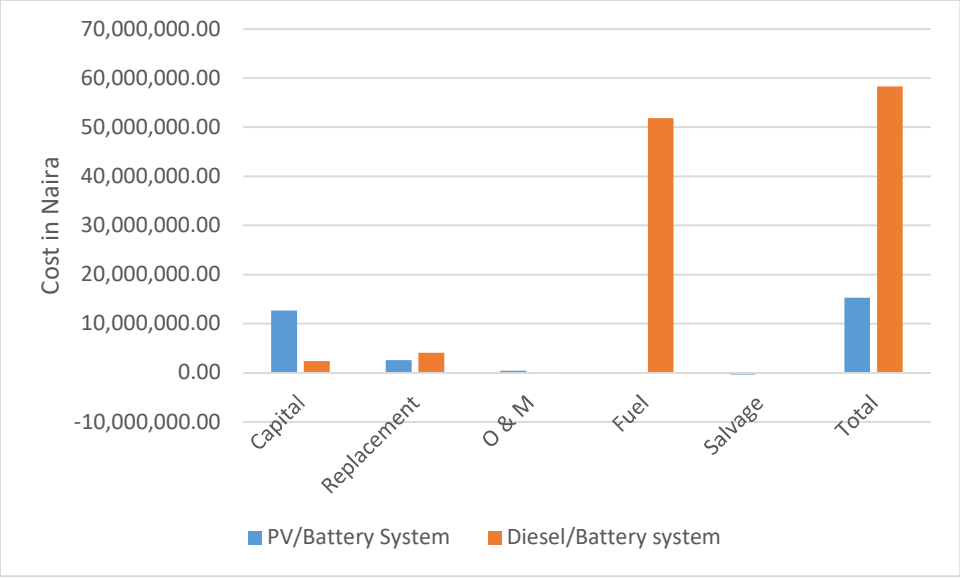



**Figure 12.** Comparison of the economics of PV system and diesel system.

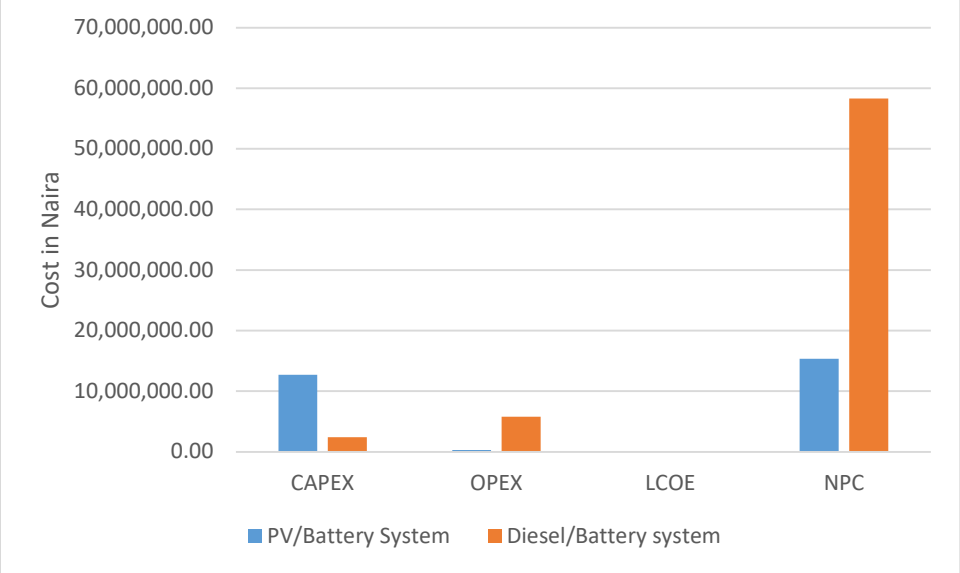



**Figure 13.** Comparison of the cost summary of the PV system and diesel system.

## 5. Conclusions

This study employed mathematical calculations to design battery storage and SPV arrays. The sizing of the PV array and battery storage was also performed using HOMER software, and the results were compared to ensure methodological consistency. The designed system met nearly all the daily electricity consumption of 23.14 kWh for a residential home by employing specific parameters: PV peak power of 8.47 kW, nominal voltage of 48 V, battery capacity of 24-unit 400 Ah batteries, charge controller capacity of 250 V/100 A, and inverter system size of 2.06 kW. In the HOMER simulation, the system architecture comprised 8.86 kW of PV, 24-unit 400 Ah batteries, a 2.29 kW inverter, and a load-following controller, collectively fulfilling the 23.14 kWh daily electricity requirement of the residential home. The manually calculated sizes for the PV and inverter, which were 8.47 kW and 2.06 kW, respectively, differed from the 8.86 kW PV and 2.29 kW inverter sizes determined by the HOMER simulation. This discrepancy is due to variations in peak load, with the manual calculation indicating a peak load of 1.32 kW, whereas the simulation showed 2.25 kW. These differences resulted from the incorporation of a 10% standard deviation in daily noise and a 20% standard deviation in hourly noise. The cost-optimal configuration resulted in a total NPC of ₦15,309,926.43 and LCOE of ₦186.81/kWh, necessitating an initial capital investment of ₦12,678,082.55. Regarding reliability, the system fulfilled nearly all annual demand, demonstrating a notably low unmet load fraction of 0.0255% and a total capacity shortage of 0.097%. Seasonal variations in solar irradiance led to an annual excess energy fraction of 36.8%, indicating potential for future integration of secondary dump loads or thermal storage. A sensitivity analysis was conducted to assess the impact of changes in solar irradiance and load growth on system performance. The results showed that the designed system methodology can be generalized to other regions of Nigeria, accommodating different climatic conditions and load profiles. The findings of this study could assist the Energy Commission of Nigeria (ECN) in formulating policies to prevent failures in off-grid SPV systems.

# Appendix A

**Table A1.** Household Load Consumption Data.

| Time (Hour) | PARLOUR | | | | | KITCHEN | | | PASSAGE | | | SECURITY/BALCONY | | | ROOM 1 | | | CHILDREN'S ROOM | | | ROOM 2 | | | ROOM 3 | | | TOILET & BATHROOM | | GRAND TOTAL |
|---|---|---|---|---|---|---|---|---|---|---|---|---|---|---|---|---|---|---|---|---|---|---|---|---|---|---|---|---|---|
| | 40 W Bulb (2) | Ceiling Fan (4) | TV Set (1) | Decoder (1) | Total (Watts) | 18 W Bulb (1) | Refrigerator (1) | Total (Watts) | Deep Freezer (1) | 18 W Bulb (1) | Total (Watts) | Security Light (6) | 18 W Bulb (1) | Total (Watts) | 18 W Bulb (1) | Ceiling Fan (1) | Total (Watts) | 18 W Bulb (1) | Ceiling Fan (1) | Total (Watts) | 18 W Bulb (1) | Ceiling Fan (1) | Total (Watts) | 18 W Bulb (1) | Ceiling Fan (1) | Total (Watts) | 18 W Bulb (2) | Total (Watts) | Overall Total (Watts-hr) |
| 0:00–1:00 | | | | | | | 300 | 300 | 300 | | 300 | 108 | | 108 | | 55 | 55 | 18 | | 18 | | 55 | 55 | | 55 | 55 | | | 891 |
| 1:00–2:00 | | | | | | | 300 | 300 | 300 | | 300 | 108 | | 108 | | 55 | 55 | 18 | | 18 | | 55 | 55 | | 55 | 55 | | | 891 |
| 2:00–3:00 | | | | | | | 300 | 300 | 300 | | 300 | 108 | | 108 | | 55 | 55 | 18 | | 18 | | 55 | 55 | | 55 | 55 | | | 891 |
| 3:00–4:00 | | | | | | | 300 | 300 | 300 | | 300 | 108 | | 108 | | 55 | 55 | 18 | | 18 | | 55 | 55 | | 55 | 55 | | | 891 |
| 4:00–5:00 | | | | | | | 300 | 300 | 300 | | 300 | 108 | | 108 | | 55 | 55 | 18 | | 18 | | 55 | 55 | | 55 | 55 | | | 891 |
| 5:00–6:00 | 80 | | | | 80 | | 300 | 300 | 300 | | 300 | 108 | | 108 | 18 | 55 | 73 | 18 | 55 | 73 | 18 | 55 | 73 | 18 | 55 | 73 | 36 | 36 | 1116 |
| 6:00–7:00 | 80 | | | | 80 | | 300 | 300 | 300 | | 300 | 108 | | 108 | 18 | 55 | 73 | 18 | 55 | 73 | 18 | 55 | 73 | 18 | 55 | 73 | 36 | 36 | 1116 |
| 7:00–8:00 | | | | | | | 300 | 300 | 300 | | 300 | | | | | | | | | | | | | | | | | | 600 |
| 8:00–9:00 | | | 90 | 21 | 111 | | 300 | 300 | 300 | | 300 | | | | | | | | | | | | | | | | | | 711 |
| 9:00–10:00 | | | 90 | 21 | 111 | | 300 | 300 | 300 | | 300 | | | | | | | | | | | | | | | | | | 711 |
| 10:00–11:00 | | | 90 | 21 | 111 | | 300 | 300 | 300 | | 300 | | | | | | | | | | | | | | | | | | 711 |
| 11:00–12:00 | | | 90 | 21 | 111 | | 300 | 300 | 300 | | 300 | | | | | | | | | | | | | | | | | | 711 |
| 12:00–13:00 | | | 90 | 21 | 111 | | 300 | 300 | 300 | | 300 | | | | | | | | | | | | | | | | | | 711 |
| 13:00–14:00 | | | 90 | 21 | 111 | | 300 | 300 | 300 | | 300 | | | | | | | | | | | | | | | | | | 711 |
| 14:00–15:00 | | | 90 | 21 | 111 | | 300 | 300 | 300 | | 300 | | | | | | | | | | | | | | | | | | 711 |
| 15:00–16:00 | | | | | | | 300 | 300 | 300 | | 300 | | | | | | | | | | | | | | | | | | 600 |

| | | | | | | | | | | | | | | | | | | | | | | | | | | | | | |
|---|---|---|---|---|---|---|---|---|---|---|---|---|---|---|---|---|---|---|---|---|---|---|---|---|---|---|---|---|---|
| 16:00–17:00 | | | | | | | 300 | 300 | 300 | | 300 | | | | | | | | | | | | | | | | | | 600 |
| 17:00–18:00 | | | | | | | 300 | 300 | 300 | | 300 | | | | | | | | | | | | | | | | | | 600 |
| 18:00–19:00 | 80 | 220 | 90 | 21 | 411 | 18 | 300 | 318 | 300 | 18 | 318 | 108 | | 108 | | | | | | | | | | | | | 36 | 36 | 1191 |
| 19:00–20:00 | 80 | 220 | 90 | 21 | 411 | 18 | 300 | 318 | 300 | 18 | 318 | 108 | 18 | 126 | | | | | | | | | | | | | 36 | 36 | 1209 |
| 20:00–21:00 | 80 | 220 | 90 | 21 | 411 | 18 | 300 | 318 | 300 | 18 | 318 | 108 | 18 | 126 | | | | 18 | 55 | 73 | 18 | | 18 | 18 | | 18 | 36 | 36 | 1318 |
| 21:00–22:00 | 80 | 220 | 90 | 21 | 411 | 18 | 300 | 318 | 300 | 18 | 318 | 108 | 18 | 126 | | | | 18 | 55 | 73 | 18 | | 18 | 18 | | 18 | 36 | 36 | 1318 |
| 22:00–23:00 | | | | | | | 300 | 300 | 300 | | 300 | 108 | | 108 | 18 | 55 | 73 | 18 | | 18 | | 55 | 55 | | 55 | 55 | 36 | 36 | 945 |
| 23:00–24:00 | | | | | | | 300 | 300 | 300 | | 300 | 108 | | 108 | 18 | 55 | 73 | 18 | | 18 | | 55 | 55 | | 55 | 55 | | | 909 |
| Total | 480 | 880 | 990 | 231 | 2581 | 72 | 7200 | 7272 | 7200 | 72 | 7272 | 1404 | 54 | 1458 | 72 | 495 | 567 | 198 | 220 | 418 | 72 | 495 | 567 | 72 | 495 | 567 | 252 | 252 | 20,954 |

## Appendix B. Cost of Key Components (Including Hardware, Installation and Labour), Interest Rate and Inflation Rate for Capital Investments

### *Appendix B.1. PV System Cost*

The cost of PV panels in the Nigerian market was estimated at ₦135,500.00 Nigerian naira (NGN), as reported by Nigerian suppliers for a module with dimensions of 1940 × 1048 × 35 mm (67.8 × 44.6 × 1.2 inches) and a peak power of output of 415 watts (Wp DC) under controlled conditions [36,37]. Expert opinion suggests an upward adjustment to ₦140,000.00 NGN to account for other support components, collectively known as balance of system (BOS) parts. These components include cables, a charge controller, lightning protection, and costs associated with delivery, labour, and installation.

### *Appendix B.2. Inverter*

According to Nigerian suppliers, the cost of a 2-kW inverter is ₦38,900.00 NGN [36,37].

### *Appendix B.3. Battery Cost*

In the Nigerian market, the price of a 12 V/400 Ah battery was reported to range from ₦390,000.00 NGN [36,37]. When considering the Balance of System (BOS) components and installation/labour costs, the total capital expenditure for the battery arrays increased to ₦400,000.00.

### *Appendix B.4. Interest Rate*

Interest rates exhibit significant variability and substantially influence cost-benefit analyses. In Nigeria, the interest rates on commercial bank loans, as determined by the Central Bank of Nigeria's Monetary Policy Rate (MPR), were recorded at 26.50% [39,40].

### *Appendix B.5. Inflation Rate*

The projected average inflation rate in Nigeria for 2026 is estimated to be between 15.51% and 16.9%. Recent data indicate a headline inflation rate of 15.90% in June 2026 [41].

## Appendix C. HOMER Design

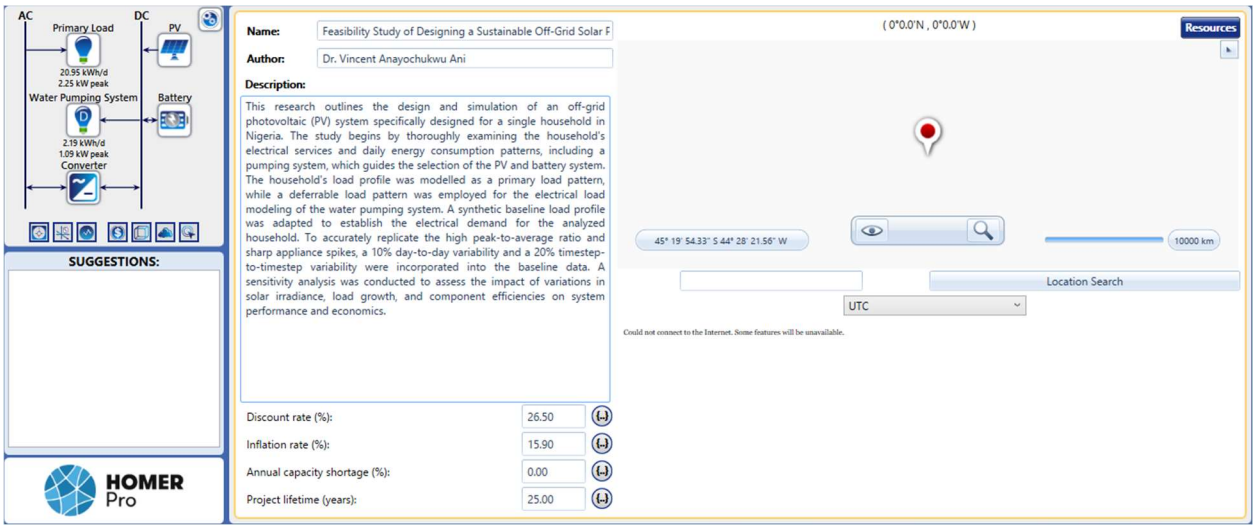



**Figure A1.** HOMER Schematic Design.

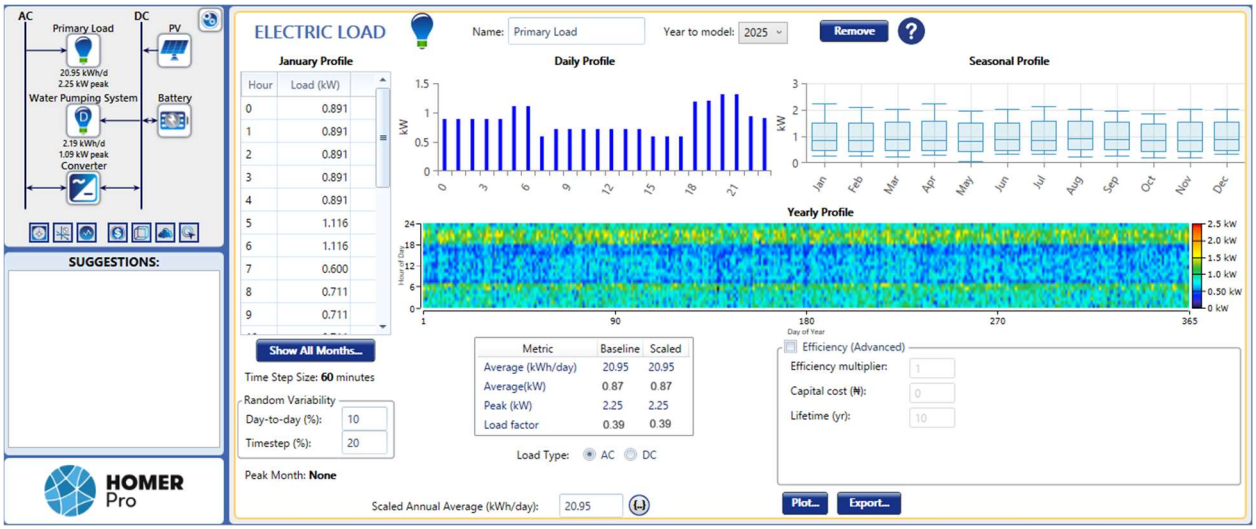



**Figure A2.** HOMER Design for Electric Load Data Input.




**Figure A3.** HOMER Design for Deferrable Load Data Input.

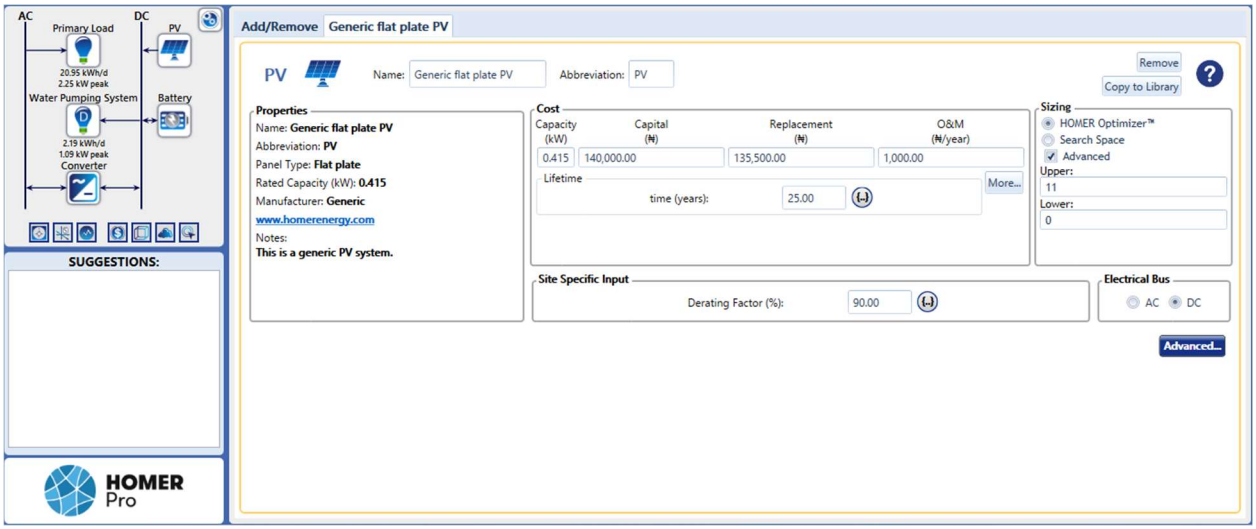



**Figure A4.** HOMER Design for PV Data Input.

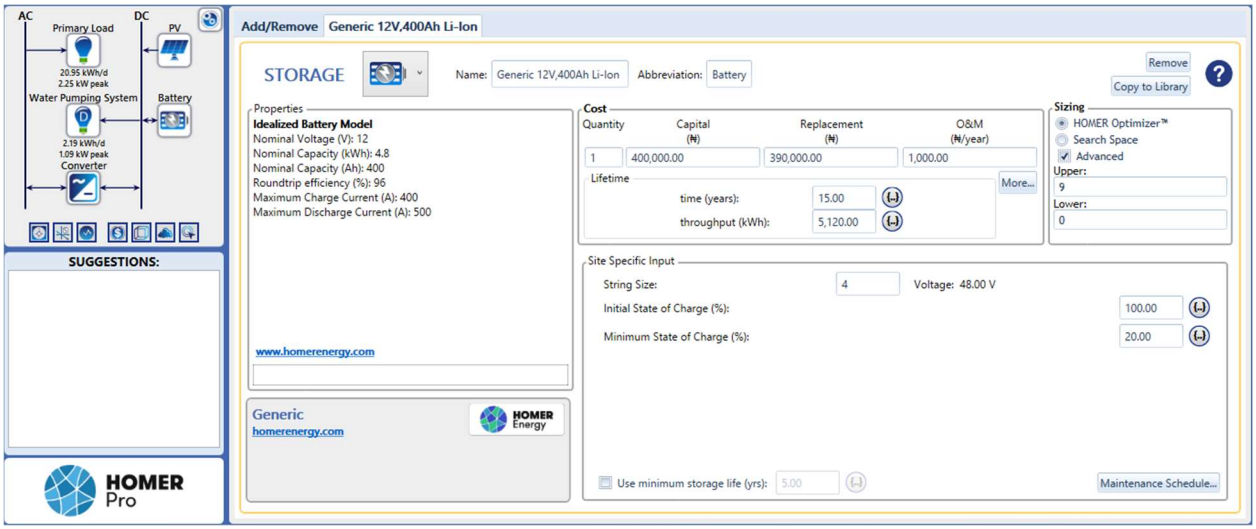



**Figure A5.** HOMER Design for Battery Data Input.

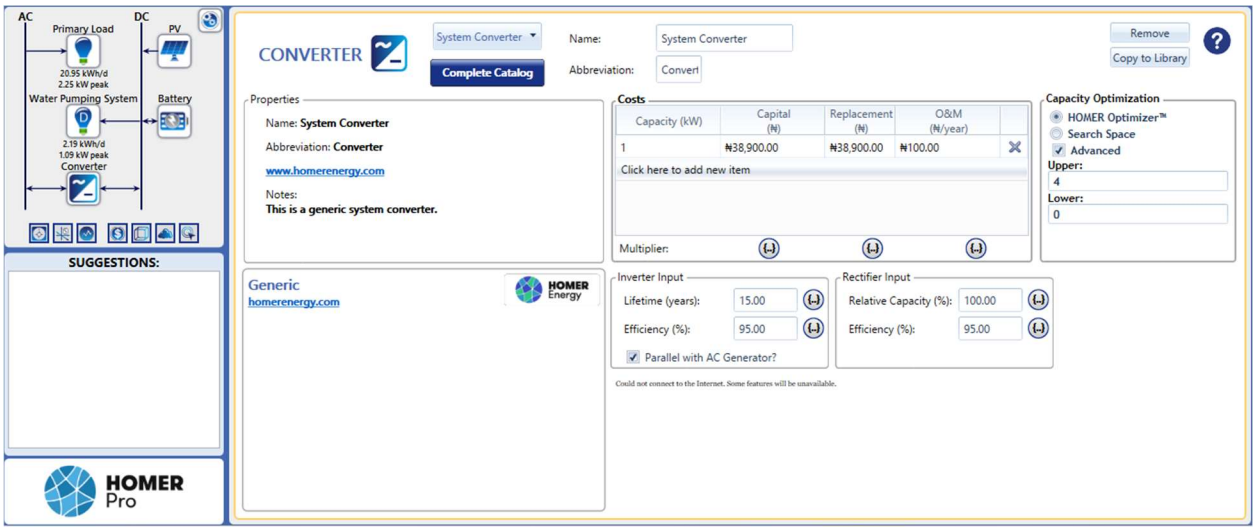



**Figure A6.** HOMER Design for Converter (Inverter) Data Input.

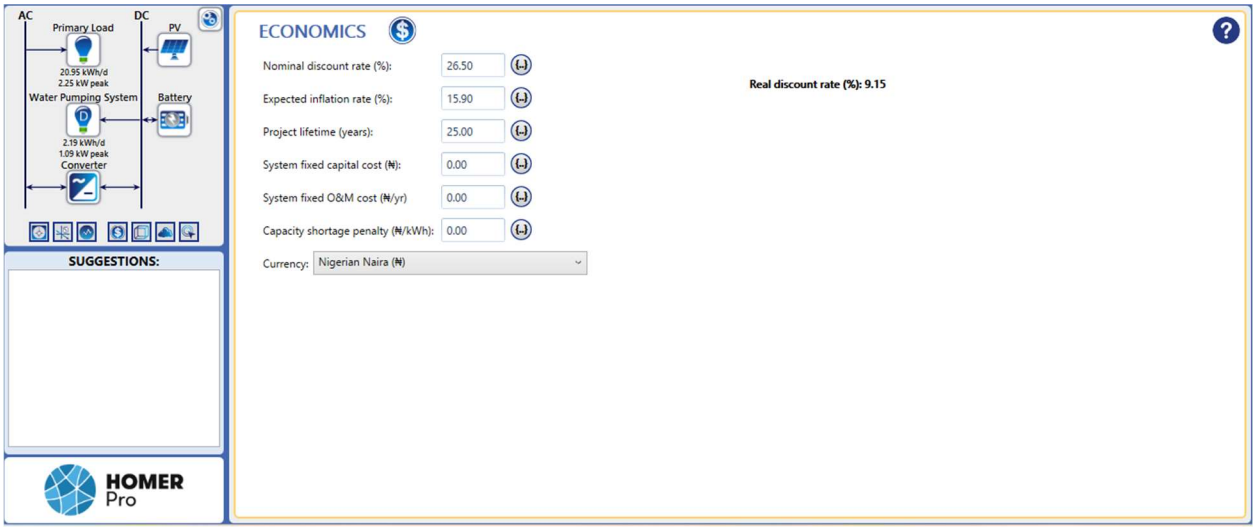



**Figure A7.** HOMER Design for Economics Data Input.

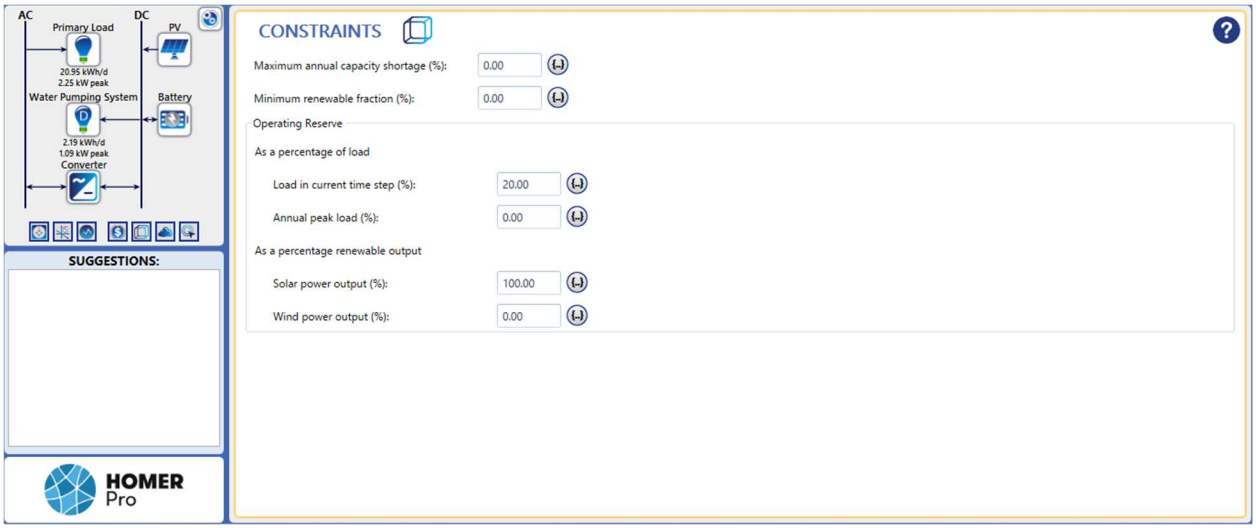



**Figure A8.** HOMER Design for Constraints Data Input.

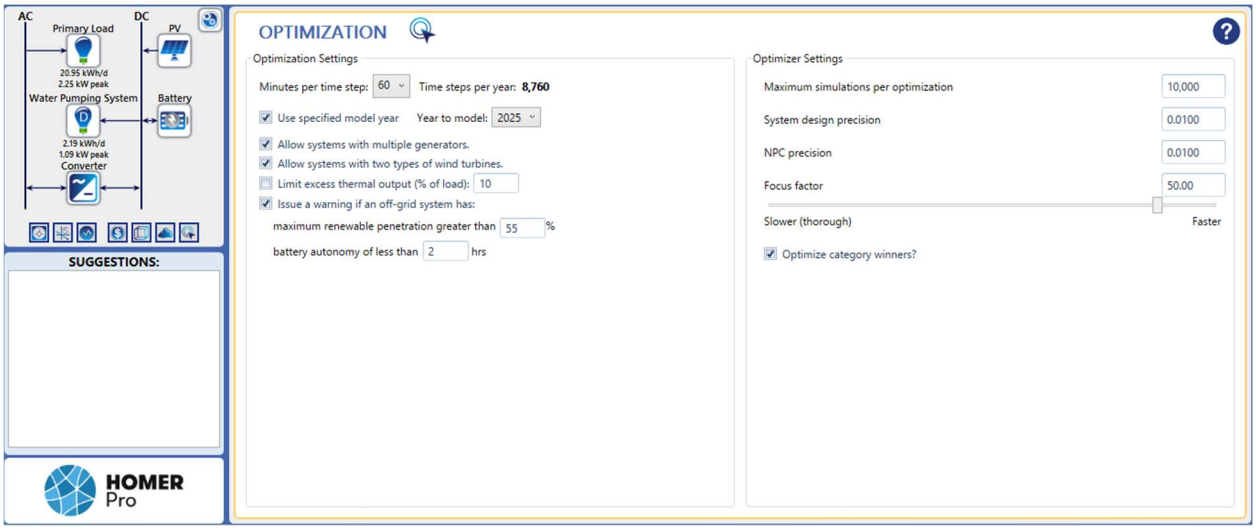



**Figure A9.** HOMER Design for Optimization Data Input.

## Author Contributions

V.A.A. conceived the study, developed the methodology, drafted the initial version of the manuscript, validated the results, analyzed the findings, and revised the manuscript. M.A. contributed to the investigation and data collection, participated in the validation process, and assisted in writing, reviewing, and editing the manuscript. All authors have reviewed and approved the final manuscript.

## Ethics Statement

Not applicable.

## Informed Consent Statement

Not applicable.

## Data Availability Statement

The data that supports the findings of this study are available on request from the authors.

## Funding

This research received no external funding.

## Declaration of Competing Interest

The authors declare that they have no known competing financial interests or personal relationships that could have appeared to influence the work reported in this paper.

## References

1. Chanchangi YN, Adu F, Ghosh A, Sundaram S, Mallick TK. Nigeria's energy review: Focusing on solar energy potential and penetration. *Environ. Dev. Sustain.* **2023**, *25*, 5755–5796. DOI:10.1007/s10668-022-02308-4
2. Adetunji F. Why Nigeria Exports Electricity to Benin Republic, Others Despite Shortfall—Energy Commission Boss, Abdullahi. Available online: https://politicalrooster.ng/why-nigeria-exports-electricity-to-benin-republic-others-despite-shortfall-energy-commission-boss-abdullahi/ (accessed on 13 August 2025).
3. Agbo EP, Edet CO, Magu TO, Njok AO, Ekpo CM, Louis H. Solar energy: A panacea for the electricity generation crisis in Nigeria. *Heliyon* **2021**, *7*, e07016. DOI:10.1016/j.heliyon.2021.e07016
4. Aboagye B, Gyamfi S, Ofosu EA, Djordjevic S. Investigation into the impacts of design, installation, operation and maintenance issues on performance and degradation of installed solar photovoltaic (PV) systems. *Energy Sustain. Dev.* **2022**, *66*, 165–176. DOI:10.1016/j.esd.2021.12.003
5. Ting SA, Rodríguez-Gallegos CD, Tay SER. Empirical investigation on the thermal behaviour of photovoltaic modules under fault conditions and localised heating. *Sol. Energy* **2026**, *310*, 114492. DOI:10.1016/j.solener.2026.114492
6. Seghiour A, Bendjeddou Y, Mostefaoui IM, Chouder A, Alharbi H, Humayd ASB, et al. Fault detection and diagnosis in photovoltaic systems using artificial intelligence and time–frequency analysis. *Sci. Rep.* **2026**, *16*, 10056. DOI:10.1038/s41598-026-39386-7
7. Mazzeo D, Colombo LPM, Leva S. A review of photovoltaic cooling with phase change materials: Technical advances, modeling approaches, efficiency gains and economic/environmental impact. *Appl. Therm. Eng.* **2025**, *280*, 128222. DOI:10.1016/j.applthermaleng.2025.128222
8. Gulkowski S. Modeling and Experimental Studies of the Photovoltaic System Performance in Climate Conditions of Poland. *Energies* **2023**, *16*, 7017. DOI:10.3390/en16207017
9. Etukudor C, Robu V, Fruh WG, Flynn D, Orovwode H. Yield assessment of Off-grid PV systems in Nigeria. In Proceedings of the 2021 IEEE PES/IAS PowerAfrica, Nairobi, Kenya, 23–27 August 2021; pp. 1–5. DOI:10.1109/PowerAfrica52236.2021.9543317
10. Yang H, Zhou W, Lou C. Optimal design and techno-economic analysis of a hybrid solar–wind power generation system. *Appl. Energy* **2009**, *86*, 163–169. DOI:10.1016/j.apenergy.2008.03.008
11. Deshmukh MK, Deshmukh SS. Modeling of hybrid renewable energy systems. *Renew. Sustain. Energy Rev.* **2008**, *12*, 235–249. DOI:10.1016/j.rser.2006.07.011
12. Abouzahr I, Ramakumar R. Loss of power supply probability of stand-alone wind electric conversion systems: A closed form solution approach. *IEEE Trans. Energy Convers.* **1990**, *5*, 445–452. DOI:10.1109/60.105267
13. Scott A, Worrall L, Hörnberg J, To LS. *How Solar Household Systems Contribute to Resilience*; Working Paper 528; Overseas Development Institute: London, UK, 2017.
14. Esan AB, Egbune D. Estimating the solar home system sizing for rural residential apartments using a panel tilt angle of 82 degrees: Ilorin, Kwara State as case study. *Electr. Comput. Eng.* **2017**, *1*, 90–96. DOI:10.13140/RG.2.2.34224.76800
15. Owusu JJ, Okoroigwe EC, Mgbemene CA, Takyi G, Ekechukwu OV. Technical stakeholders' perspective of solar photovoltaic system failure in Sub-Saharan Africa: The case of Ghana. *Sustinere J. Environ. Sustain.* **2025**, *9*, 24–40. DOI:10.22515/sustinere.jes.v9i1.431
16. Garo FS. A Study of the Challenges in Adoption of Renewable Energy in Nigeria. Doctoral Thesis, University of Lancashire, Preston, UK, 2025. DOI:10.17030/uclan.thesis.00058865
17. Ali W, Farooq H, Rehman AU, Awais Q, Jamil M, Noman A. Design considerations of stand-alone solar photovoltaic systems. In Proceedings of the 2018 International Conference on Computing, Electronic and Electrical Engineering (ICE Cube), Quetta, Pakistan, 12–13 November 2018; pp. 1–6. DOI:10.1109/ICECUBE.2018.8610970
18. Nyangoka IK. A Framework for Sizing Solar PV Systems Adaptable to Off Grid Areas. Ph.D. Dissertation, Strathmore University, Nairobi, Kenya, 2024. Available online: http://hdl.handle.net/11071/15688 (accessed on 12 January 2026).
19. Ogunsiji GO, Alabi OO, Akande TO. Energy Storage Solutions for Enhanced Performance in Off-Grid Solar Systems in

Abuja, Nigeria. *J. China Univ. Min. Technol.* **2024**, *29*, 49–61. Available online: https://zkdx.ch/journal/zkdx/article/view/53 (accessed on 12 January 2026).
20. Ashton C, Siira M. IEEE Recommended Practice for Sizing Stand-Alone Photovoltaic (PV) Systems. In *IEEE Std 1562–2021 (Revision of IEEE Std 1562–2007)*; IEEE: Piscataway, NJ, USA, 2021; pp. 1–35. DOI:10.1109/IEEESTD.2021.9528316
21. Adewuyi OB, Kiptoo MK, Afolayan AF, Amara T, Alawode OI, Senjyu T. Challenges and prospects of Nigeria's sustainable energy transition with lessons from other countries' experiences. *Energy Rep.* **2020**, *6*, 993–1009. DOI:10.1016/j.egyr.2020.04.022
22. Egbon OC. Optimal Sizing of a Standalone Photovoltaic (PV) System for Residential Customers Considering Electricity Consumption Patterns: A Case Study of Ibadan City, Nigeria. Master's Thesis, School of Engineering, Auckland University of Technology, Auckland, New Zealand, 2019. Available online: https://hdl.handle.net/10292/12977 (accessed on 12 January 2026).
23. Ahmad GE. Photovoltaic-powered rural zone family house in Egypt. *Renew. Energy* **2002**, *26*, 379–390. DOI:10.1016/S0960-1481(01)00131-8
24. Al-Salaymeh A, Al-Hamamre Z, Sharaf F, Abdelkader MR. Technical and economical assessment of the utilization of photovoltaic systems in residential buildings: The case of Jordan. *Energy Convers. Manag.* **2010**, *51*, 1719–1726. DOI:10.1016/j.enconman.2009.11.026
25. Kaushika ND, Rai AK. Solar PV design aid expert system. *Sol. Energy Mater. Sol. Cells* **2006**, *90*, 2829–2845. DOI:10.1016/j.solmat.2006.04.010
26. Ani VA. Design of a Stand-Alone Photovoltaic Model for Home Lightings and Clean Environment. *Front. Energy Res.* **2016**, *3*, 54. DOI:10.3389/fenrg.2015.00054
27. Ezike EC, Nwobodo AN. Groundwater Potential of Akpugo in Nkanu Area Enugu, Southeastern Nigeria. *Int. J. Adv. Sci. Tech. Res.* **2021**, *6*, 21–30. Available online: https://www.researchgate.net/profile/Hkay-Hubs-2/publication/357635334_Groundwater_Potential_Of_Akpugo_In_Nkanu_Area_Enugu_Southeastern_Nigeria/links/66e136232390e50b2c7e869f/Groundwater-Potential-Of-Akpugo-In-Nkanu-Area-Enugu-Southeastern-Nigeria.pdf (accessed on 12 January 2026).
28. Ubuy Nigeria. Grundfos 11 SQF-2 SQFlex Solar Water Pump. Available online: https://www.u-buy.com.ng/product/2FNEA1U8-grundfos-11-sqf-2-sqflex-solar-water-pump (accessed on 15 October 2026).
29. Grundfos Product-Selection. Grundfos 11 SQF-2 SQFlex Solar Submersible Pump. Available online: https://product-selection.grundfos.com/ca/products/sqflex/11-sqf-2-96078029?pumpsystemid=3005610934&tab=variant-curves (accessed on 12 January 2026).
30. Sara ID, Rosmin N, Bahi M, Zulkepli MDM. Design and sizing of stand-alone photovoltaic systems for remote areas. *J. Energy Saf. Technol.* **2024**, *7*, 130–141. DOI:10.11113/jest.v7.187
31. Ani VA. Development of a stand-alone photovoltaic (PV) energy system with multi-storage units for sustainable power supply. *Renew. Energy Environ. Sustain.* **2024**, *9*, 10. DOI:10.1051/rees/2024007
32. HOMER Energy. *HOMER Pro Microgrid Analysis Sizing Software (v3.16)—Sensitivity Analysis and Optimization Algorithms User Guide*; HOMER Energy LLC: Boulder, CO, USA, 2024.
33. Lambert T, Gilman P, Lilienthal P. Micropower System Modeling with Homer. In *Integration of Alternative Sources of Energy*; Farret FA, Simões MG, Eds.; Wiley: Hoboken, NJ, USA, 2006; Volume 1, pp. 379–385. DOI:10.1002/0471755621.ch15
34. National Renewable Energy Laboratory (NREL). *Solar Position and Intensity Calculations for Sizing Standalone Photovoltaic Systems*; Technical Report NREL/TP-5500-84321; NREL: Golden, CO, USA, 2023.
35. HOMER Energy. HOMER® Pro Version 3.7 User Manual. 2016. Available online: https://homerenergy.com/static/pdf/HOMERHelpManual.pdf (accessed on 12 January 2026).
36. Jiji Nigeria. 2026. Available online: https://jiji.ng/ojo/power-equipments/ (accessed on 12 January 2026).
37. Gennex Technologies. 2026. Available online: https://gennextechnologies.com/ (accessed on 12 January 2026).
38. Liao R, Manfren M, Nastasi B. Off-grid PV systems modelling and optimisation for rural communities—Leveraging understandability and interpretability of modelling tools. *Energy* **2025**, *324*, 135948. DOI:10.1016/j.energy.2025.135948
39. Monetary Policy Decisions. 2026. Available online: https://www.cbn.gov.ng/MonetaryPolicy/decisions.html (accessed on 12 January 2026).
40. Nigeria Interest Rate. 2026. Available online: https://tradingeconomics.com/nigeria/interest-rate (accessed on 12 January 2026).
41. Nigeria Inflation Rate. 2026. Available online: https://tradingeconomics.com/nigeria/inflation-cpi (accessed on 12 January 2026).